AD-A180 862 SKY POLARIZATION DATA FOR VOLCANIC AND NON-VOLCANIC PERIODS(U) OPTIMETRICS INC BURLINGTON MA D R LONGTIN ET AL. OCT 86 OMI-180 AFGL-TR-86-0223 1/1

UNCLASSIFIED F19628-85-C-0178 F/G 4/1 NL

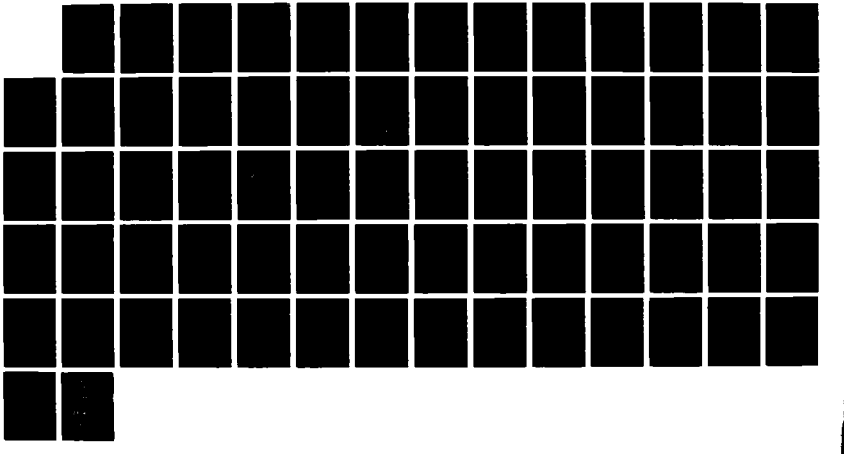

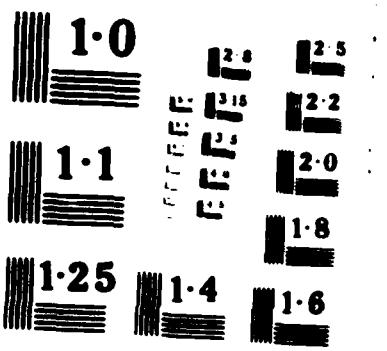
1·0
1·1
1·25
1·4
2·5
2·2
2·0
1·8
1·6

AFGL-TR-86-0223 OMI-180

Sky Polarization Data for Volcanic and Non-Volcanic Periods

David R. Longtin
Frederic E. Volz

OptiMetrics
121 Middlesex Turnpike
Burlington, MA 01803-4998

October 1986

Scientific Report No. 3

AIR FORCE GEOPHYSICS LABORATORY
AIR FORCE SYSTEMS COMMAND
UNITED STATES AIR FORCE
HANSCOM AIR FORCE BASE, MASSACHUSETTS 01731

SECURITY CLASSIFICATION OF THIS PAGE

REPORT DOCUMENTATION PAGE

1a. REPORT SECURITY CLASSIFICATION Unclassified	1b. RESTRICTIVE MARKINGS
2a. SECURITY CLASSIFICATION AUTHORITY	3. DISTRIBUTION / AVAILABILITY OF REPORT approved for public release; distribution unlimited
2b. DECLASSIFICATION / DOWNGRADING SCHEDULE	
4. PERFORMING ORGANIZATION REPORT NUMBER(S) OMI-180	5. MONITORING ORGANIZATION REPORT NUMBER(S) AFGL-TR-86-0223
6a. NAME OF PERFORMING ORGANIZATION OptiMetrics, Inc. — 6b. OFFICE SYMBOL (If applicable)	7a. NAME OF MONITORING ORGANIZATION Air Force Geophysics Laboratory
6c. ADDRESS (City, State, and ZIP Code) 121 Middlesex Turnpike Burlington, Massachusetts 01803-4998	7b. ADDRESS (City, State, and ZIP Code) Hanscom Air Force Base, Massachusetts 01731
8a. NAME OF FUNDING / SPONSORING ORGANIZATION — 8b. OFFICE SYMBOL (If applicable)	9. PROCUREMENT INSTRUMENT IDENTIFICATION NUMBER F19628-85-C-0178
8c. ADDRESS (City, State, and ZIP Code)	10. SOURCE OF FUNDING NUMBERS

PROGRAM ELEMENT NO.	PROJECT NO.	TASK NO.	WORK UNIT ACCESSION NO
62101F	7670	15	AI

11. TITLE (Include Security Classification)

Sky Polarization Data for Volcanic and Nonvolcanic Periods

12. PERSONAL AUTHOR(S)
David R. Longtin Frederic E. Volz*

13a. TYPE OF REPORT	13b. TIME COVERED	14. DATE OF REPORT (Year, Month, Day)	15. PAGE COUNT
Scientific #3	FROM 4/86 TO 9/86	October 1986	72

16. SUPPLEMENTARY NOTATION

*AFGL/OPA, Hanscom AFB, MA 01731

17 COSATI CODES			18. SUBJECT TERMS (Continue on reverse if necessary and identify by block number)
FIELD	GROUP	SUB-GROUP	Turbidity, aerosol, El Chichon eruption Neutral point, sky polarization, volcanic aerosol, Arago point, Babinet point, Mt. Pelee

19. ABSTRACT (Continue on reverse if necessary and identify by block number)

Volz has monitored the Arago and Babinet neutral points at Lexington and Bedford, Mass. for the years 1968 to 1986. These data, along with measurements of turbidity, twilight color ratio, solar aureole and cloud and snow cover, have been assembled into a database and checked for error. The neutral point data were then corrected for day to day variations in tropospheric turbidity and separated into groups which coincide with time periods of known volcanic influences and seasonal events. 3-D plots indicate that both the Arago and Babinet points were strongly affected by the presence of the El Chichon dust cloud; however, the features were not as pronounced as in the tropics. Measurements made after the El Chichon eruption also suggest a movement of the neutral points after sunset which was not observed after the eruptions of Mt. Pelee in 1902 and Katmai in 1911. The present measurements did not show an effect from the eruptions of Fuego in 1971 and late 1974.

20. DISTRIBUTION / AVAILABILITY OF ABSTRACT	21. ABSTRACT SECURITY CLASSIFICATION
☐ UNCLASSIFIED/UNLIMITED ☐ SAME AS RPT ☐ DTIC USERS	Unclassified

22a. NAME OF RESPONSIBLE INDIVIDUAL	22b. TELEPHONE (Include Area Code)	22c. OFFICE SYMBOL
Eric Shettle		AFGL/OPA

DD FORM 1473, 84 MAR — 83 APR edition may be used until exhausted. All other editions are obsolete.

SECURITY CLASSIFICATION OF THIS PAGE

CONTENTS

Illustrations

Tables

1. INTRODUCTION

There are many methods available to monitor atmospheric aerosols near the ground and in the stratosphere where volcanic dust may remain for years. The technique of interest to this report involves the measurement of neutral points, directions in the solar vertical where skylight is unpolarized. Many measurements of sky polarization, especially the position of the neutral points, have been made since 1886 after the eruption of Krakatoa. Regarded as one of the first objective methods used to study the properties of atmospheric aerosols, the position of the neutral points shows seasonal variations and strong deviations during highly volcanic periods. Recently, extreme results were obtained in late 1982 in Hawaii following El Chichon's eruption.

Using customary visual observations, Volz has monitored the position of neutral points known as the Arago and Babinet points from Bedford and Lexington, Massachusetts. A third neutral point called the Brewster point is more difficult to observe and will not be discussed in this report. The data encompass an 18 year period beginning in 1968 and, therefore, provide an excellent opportunity to study how neutral points respond to varying tropospheric turbidity and layers of stratospheric dust. Although not the aim of this report, these new observations might, on the basis of good knowledge of aerosol parameters and theoretical tools, be

used to interpret the historical record of neutral points Sekera[1], Jensen[2].

1.1 Organization of the Report

The present effort is a partial evaluation of the series of observations made by Volz. Chapter 2 presents a brief discussion of the nature of Arago and Babinet points. Chapter 3 presents the contents and organization of the neutral point database--key material for the present study. Chapter 4 discusses the effects of tropospheric turbidity, sea surface reflections and snow cover on the neutral point data. Chapter 5 describes the method of removing the effects of tropospheric turbidity on the position of neutral points. These turbidity corrections are necessary because the movement of neutral points resulting from day-to-day changes in turbidity may overshadow any movement caused by stratospheric aerosols. Until now, such corrections could not be made because turbidity was not an accurately measured quantity. In Chapter 6, the neutral point data is presented in a manner which reveals their complex behavior in response to the injection of volcanic dust into the stratosphere. It specifically focuses on the eruptions of Fuego in 1974 and 1978, and of El Chichon in 1982. Chapter 6 also includes a brief comparison of the measurements made by Volz with those

1. Sekera, Z. (1956) Recent developments in the study of the polarization of skylight, in Advances in Geophysics, Academic Press, Inc., New York, 3:43-104.
2. Jensen, C. (1957) Die Polarisation des Himmelslichtes, in Handbuch der Geophysik, Borntraeger, Berlin, 8:527-620.

from other researchers. Finally, Chapter 7 summarizes our results.

2. THE ARAGO AND BABINET POINTS

2.1 Explanation of the Neutral Points

Arago and Babinet points result from the interplay between primary and higher-order scattered sunlight. Insight can be gained into why these neutral points are observed through the following argument. First, consider a single scattering atmosphere composed entirely of small spherical particles. Here, one would observe nearly unpolarized light when looking very close to the sun. This is because sunlight is unpolarized and as a result, the light scattered in the forward direction by spherical particles will be unpolarized also. Now consider an atmosphere where higher-order scattering is important. This time, an observer looking towards the sun will see light which has been scattered at least once from angles other than forward direction. Because this light is, in general, partially polarized, the observer will measure partially polarized light when looking near the sun. Extending the argument a little further, the addition of the multiple-scattered to primary-scattered light (having a different state of polarization), will lead to zero polarization being observed at other locations in the sky. Specifically, the Babinet point is usually found about 20 degrees above the sun and the Arago point (only observable when the sun is low in the sky), is about 20 degrees above the anti-

solar point. Calculations by Chandrasekhar[3], which incorporate higher-order scattering into a Rayleigh atmosphere, confirm the presence of Arago and Babinet points. Extended calculations have been performed by Coulson et al[4].

2.2 Factors Influencing Neutral Points

Intuitively, one would expect the Arago and Babinet points to depend on the vertical distribution and the optical depth of the scattering aerosol. The first factor will be important especially when a volcanic dust layer is present. For a Rayleigh atmosphere, the effect of optical depth on neutral points has been investigated by Holzworth and Rao[5] using the calculations by Coulson et al[4]. They have shown that both the Arago and Babinet points increase as optical depth increases. Consequently, one would expect the position of neutral points to depend on the solar elevation angle because the optical depth of the atmosphere is a function of solar elevation angle. In addition, assuming that aerosols have similar effects as air molecules, one may expect a seasonal variation in the position of neutral points. This is because a summer sky is usually hazier than the winter sky.

3. Chandrasekhar, S. (1950) Radiative Transfer, Oxford University Press.
4. Coulson, K.L., Dave J.V., and Sekera Z. (1960) Tables Related to Radiation Emerging from a Planetary Atmosphere with Rayleigh Scattering, University of California Press, Berkley and Los Angeles.
5. Holzworth, G., and Rao C.R.N. (1965) Studies of skylight polarization, J. Opt. Soc. Am. 55:403-408.

Because multiple scattering is very much influenced by reflection phenomena, the presence of clouds and the type of ground surface (snow or water, in particular) may also affect the position of neutral points. These effects cause noise in the data and put restraints on interpretation.

2.3 Measurement of Neutral Points

The neutral point data were taken at two locations because the time of day for twilight and dawn vary greatly over the year. The Air Force Geophysics Laboratory (AFGL), where observations down to the horizon were possible, was the site of most weekday observations during the winter. Measurements were also made at the Volz home. At this location, however, neutral points normally could not be observed if their elevation angle was smaller than 7 to 14 degrees. In important situations, such as the presence of volcanic clouds, attempts were made to find better locations for the observations.

The neutral points were found with a visual polariscope that uses a Savart prism as a polarizer and a colorless Polaroid filter as an analyzer. When viewed through this instrument, the neutral points appear as a gap in the polarization fringes commonly known as a "bridge." A pendulum with an elevation angle scale has been mounted on the instrument so that when a neutral point is in the line of sight, its elevation can be read instantly. Errors associated with this measurement technique are 0.5 degrees for the

Arago point and 1.0 degrees for the Babinet point, but very weak fringes sometimes caused larger errors.

The primary data were obtained by measuring the angle between the horizontal direction and each neutral point as a function of time, that is, at odd solar elevation angles. Since it is customary to express the Arago and Babinet points as the angle between zero polarization and the anti-solar and solar direction respectively, the elevation angles of the Arago and Babinet points were converted to solar distances:

$$DA = \text{Arago elevation angle} + H$$

and

$$DB = \text{Babinet elevation angle} - H,$$

where H is the unrefracted solar elevation angle associated with a particular observation of a Arago or Babinet point (see Figure 1). Hereafter, any reference to the Arago and Babinet points will be in terms of DA and DB unless stated otherwise. DA and DB were then plotted against the solar elevation angle for angles between +20 to -6 degrees and the values at nine fixed solar elevations were determined by linear interpolation. For the purpose of analyzing the data, it was helpful to also calculate the difference, DBA = DB-DA. Figure 2 provides an example of these plots using data representative of nonvolcanic periods. The data and plots were then carefully checked for error. Since the interpolation was made irrespective of large gaps in H, improper values were removed. Also, extrapolation over not

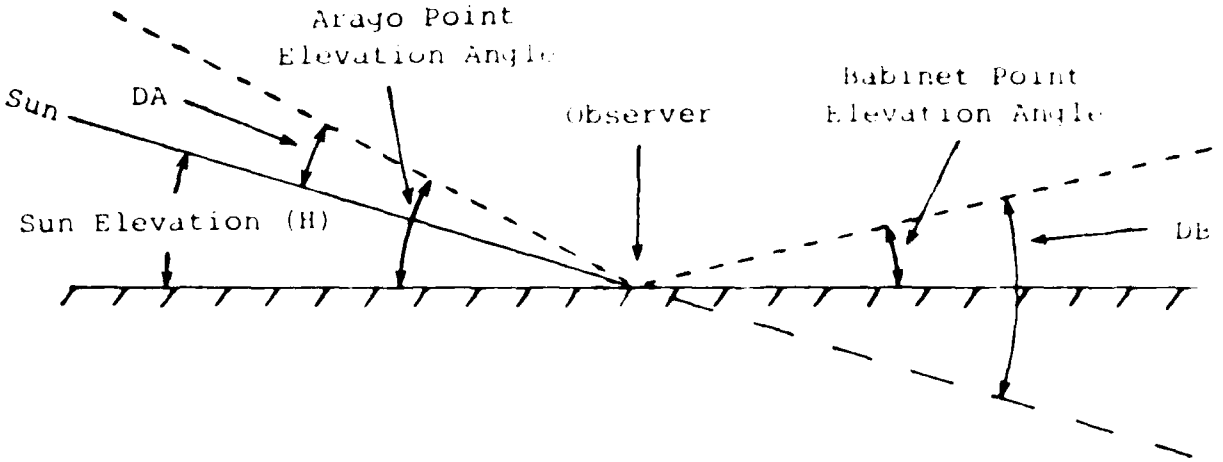

Figure 1. Arago and Babinet Points in the Solar Vertical

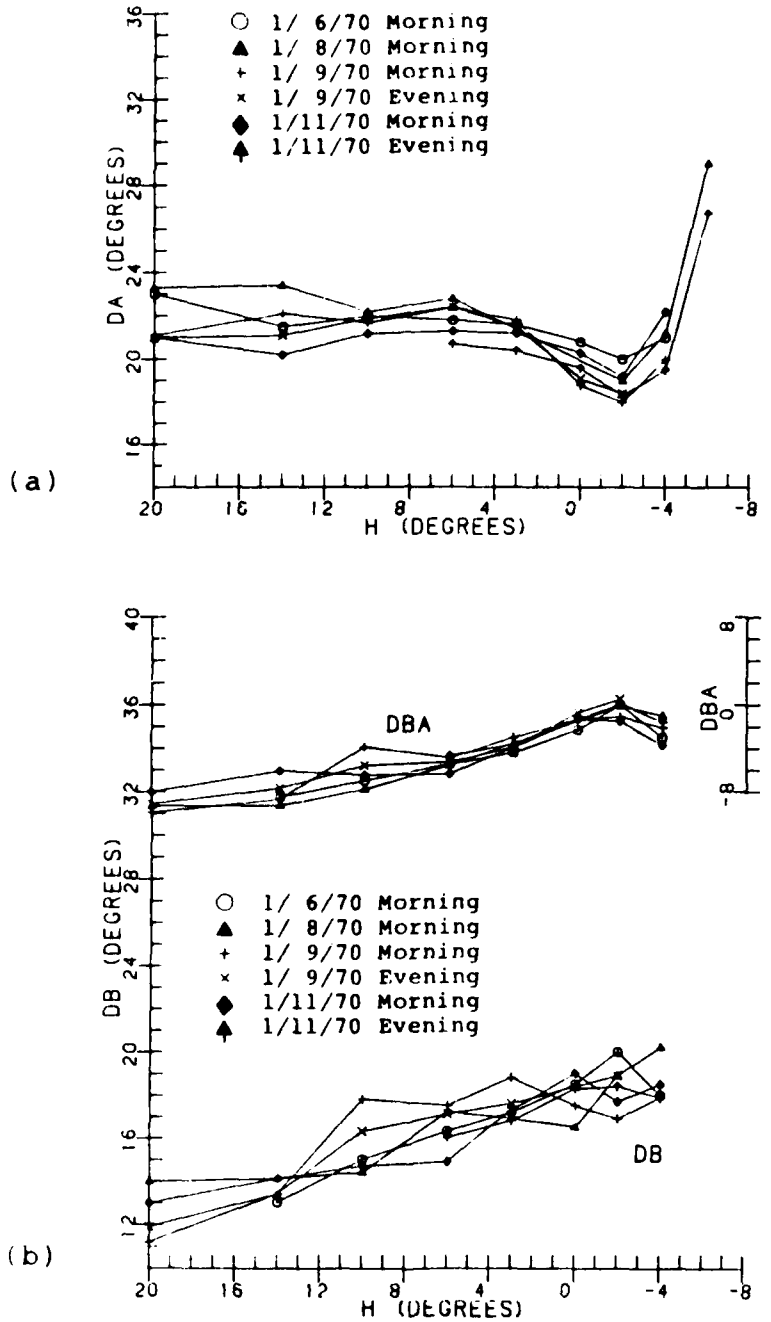

Figure 2. Values of DA, DB, and DBA at Fixed Solar Elevation Angles for Selected Days Between January 6, 1970 and January 11, 1970. These Data Are Representative of Nonvolcanic Time Periods. Note the DBA Scale Is Twice the Scale of DA and DB

more than 2 degrees in solar elevation was added where warranted.

The new data file for fixed H is the subject of the present work. The choice of the fixed H angles reproduces the course of the original observations very well except for the times when the volcanic influence caused DA and DB to change rapidly as a function of solar elevation angle. This volcanic effect on DA and DB was observed only after the arrival of the El Chichon dust cloud (see Figure 3). Near sunrise and sunset, better agreement between the primary data and the interpolated values would have resulted if an additional fixed solar angle of 1.5 degrees had been used. The El Chichon effect also caused the measurements at a given H to change considerably from set to set until late 1984.

3. THE DATABASE

3.1 Neutral Points

The database consists of approximately 1300 sets of observations in all. Each set contains values for DA and DB at some or all of the following solar elevation angles: 20, 14, 10, 6, 3, 0, -2, -4 and -6 degrees. Measurements were taken both in the morning (M) and in the evening (E), and have been noted accordingly. The data encompass the time period extending from October 1968 to June 1986, but there is a large gap from 1977 to 1980 when no measurements were taken. Furthermore, the observations are spurious in nature and tend to occur in groups of a few clear days because observa-

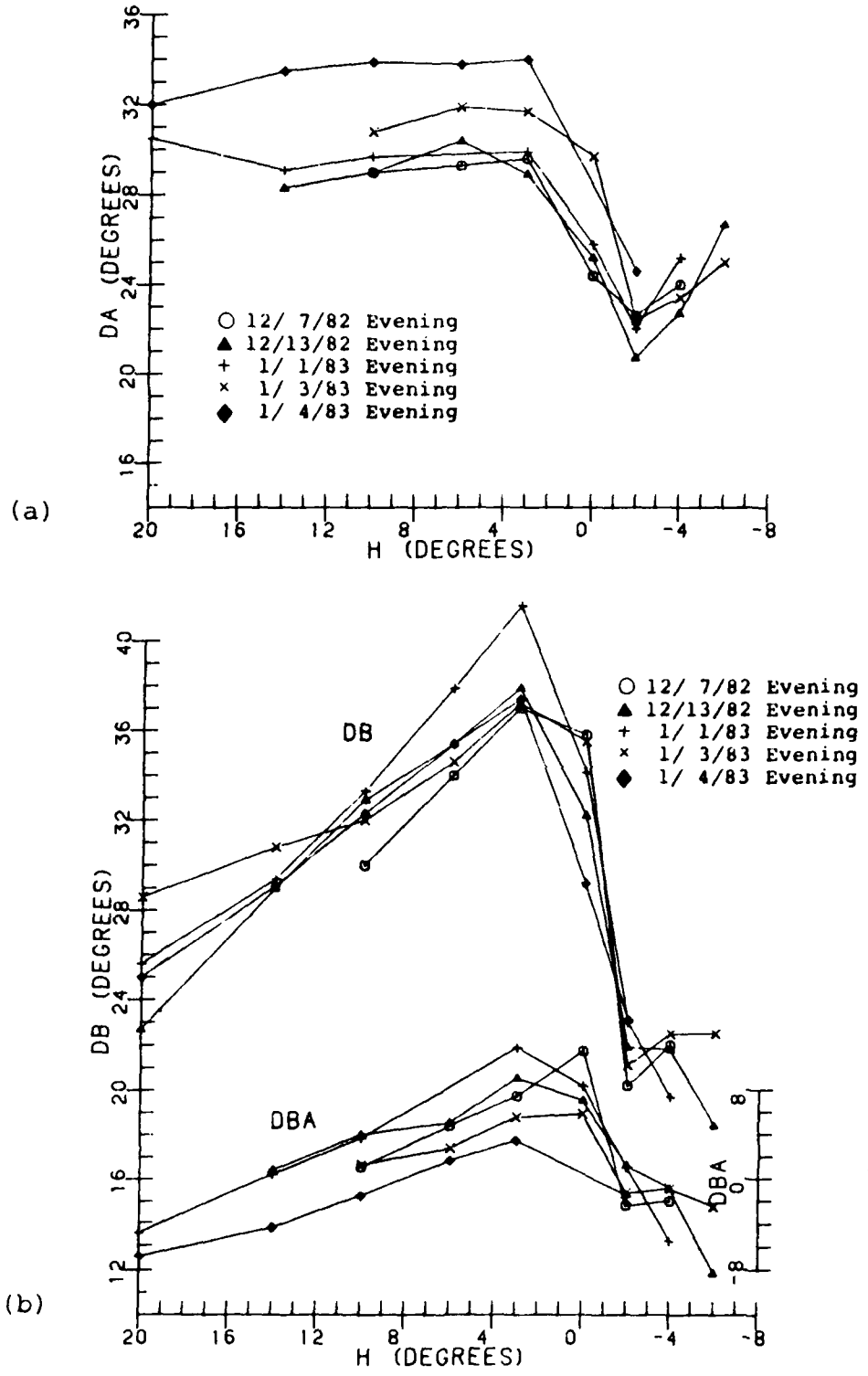

Figure 3. The El Chichon Effect on (a) DA and (b) DB and DBA for Selected Days Between December 7, 1982 and January 4, 1983

tions can only be made in essentially cloud-free conditions. Figure 4 shows the number of morning and evening observations as a function of month and year.

3.2 Other Parameters

In addition to the neutral point data, six parameters are included which attempt to characterize the optical state of the atmosphere: atmospheric turbidity, turbidity type, cloud conditions and snow cover, solar aureole and the logarithm of the ratio of red to green light in the twilight sky. These parameters could prove helpful when analyzing the neutral point data. Atmospheric turbidity, plus cloud and snow cover are described below because they are of some interest to the current work. The other parameters are summarized in the Appendix.

3.2.1 Atmospheric Turbidity

In this report, the term "atmospheric turbidity" will refer to the aerosol optical density (B) at a wavelength of 500 microns. The aerosol optical density is related to the aerosol optical thickness by

$$B = \text{Aerosol Optical Thickness}/2.30.$$

Values for B were obtained by means of sun photometer measurements of the solar intensity. The measurements were generally taken shortly before sunset or after sunrise. In some cases however, the values had to be estimated from noontime

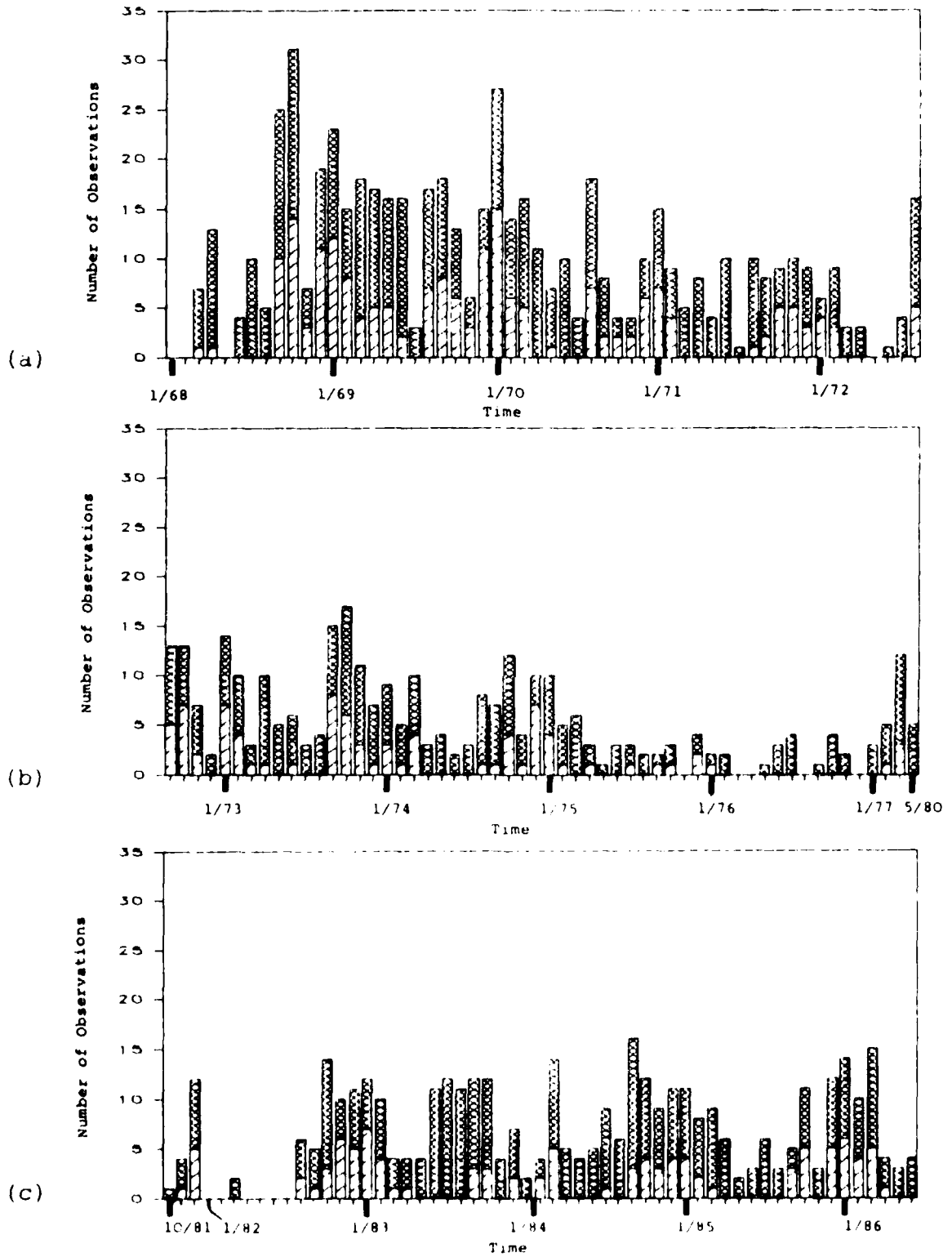

Figure 4. Number of Morning (Single Slashed Bar) and Evening (Cross Hatched Bar) Observations per Month from (a) Jan. 68 to Aug. 1972, (b) Sept. 1972 to May 1980, and (c) Oct. 1982 to June 1986

measurements because of cloud and horizon conditions. For values of B less than 0.1, the error in the B is 0.01 in magnitude and for higher turbidities, it is 10% of the value of B.

3.2.2 Cloud Condition and Snow Cover

As a rule, measurements were taken only when the local sky was nearly free of clouds. Small transient clouds were tolerated as long as they were not in immediate vicinity of the neutral points. The presence of clouds and snow cover are coded in the database according to the numbering scheme described in Table 1. A value for the cloud condition was chosen so that it represented the average cloud cover observed during the course of a whole set of morning or evening measurements. Also, the code numbers from 50 to 53 indicate that the snow cover, within 10 km of the observation site, was estimated to be at least 30%.

3.3 Organization of the Database

Before the neutral point data could be analyzed, it was necessary to update the existing data with additional data provided by Volz and to then reorganize the database. The first task was done by merging a data file composed entirely of new data with original data. The new data consisted of additional measurements of the neutral points and the optical parameters discussed in previous section. A unified data format was then developed because the original data had been

Table 1. Cloud and Snow Cover Codes Used in the Neutral Point Database

Code Number	Observed Condition *
00	No Clouds
01	Clouds less than 5 degrees above the horizon in the direction opposite to the sun
02	Clouds less than 10 degrees above the horizon in the direction opposite to the sun
10	Thin cirrus less than 5 degrees above the horizon in the direction of the sun
11	Thin cirrus and altocumulus less than 10 degrees above the horizon in the direction of the sun
12	More dense clouds less than 10 degrees in the direction of the sun
22	Clouds less than 10 degrees above the horizon at all azimuthal angles
33	Same as code 22 plus scattered clouds higher up
34	Clouds all over sky, but less than 5/8 coverage
40	Cirrus and haze over much of sky
50	Snow cover, cloudless skies
51	Snow cover, plus the sky conditions in codes 11, 12, and 22
52	Snow cover, plus the sky conditions in code 33
53	Snow cover, plus the sky conditions in code 34

* From 1974 to 1986 no observations were made during cloudy conditions described by code numbers 12 to 34, 52, and 53

given in different formats. The new format permits easier access to the data when performing statistical and graphing tasks. An example of the newly adopted format is given in Table 2. Each line corresponds to a particular date when neutral point data were taken. Missing neutral point data are represented by zeros.

At this point, the data were checked as much as possible for errors (i.e. duplicate records, typos, obviously wrong data, etc.). Also, any observations made at locations other than Bedford or Lexington, Massachusetts were withdrawn. This is why some line numbers do not contain data.

4. THE EFFECTS OF VARIOUS OPTICAL PARAMETERS ON THE NEUTRAL POINT DATA

4.1 Atmospheric Turbidity

As mentioned in Chapter 2, the amount of scattering by aerosols will affect the position of the neutral points. To determine the extent of this effect, scatter plots of the neutral point data as a function of the observed atmospheric turbidity were constructed. Separate plots were made for DA and DB, and for each fixed solar elevation angle. When making the scatter plots, only the data taken prior to the arrival of the El Chichon dust cloud were used because it was clear that the presence of the cloud altered the location of the neutral points much more than changes in tropospheric turbidity (and in a way that was different from the turbidity influence).

Table 2. Format of the Neutral Point Database

No.	Yr	Day	Mo	M/E	Arago Points (DA) For Solar Elevation Angles From 20 to -6 Degrees									Babinet Points (DB) For Solar Elevation Angles From 20 to -6 Degrees									Other Parameters*				
					20	14	10	6	3	0	-2	-4	-6	20	14	10	6	3	0	-2	-4	-6	B	TT	CL	A	LCR
272	69	9	9	E	.0	.0	.0	.0	.0	21.5	.0	21.8	.0	.0	.0	.0	.0	.0	.0	.0	18.7	.0	.150		0		
273	69	10	9	M	.0	21.0	.0	.0	.0	.0	.0	.0	.0	.0	8.5	.0	.0	.0	.0	.0	.0	.0	.050		0		
274	69	11	9	M	19.4	19.4	19.7	20.9	20.3	20.0	.0	.0	.0	.0	6.0	8.2	10.0	15.0	15.5	.0	.0	.0	.020		0		
275	69	11	9	E	.0	.0	.0	23.0	.0	.0	.0	.0	.0	.0	.0	.0	18.0	.0	.0	.0	.0	.0	.100		22		
276	69	12	9	E	.0	26.2	25.6	24.6	23.0	21.7	21.0	22.0	25.0	.0	14.5	16.0	18.8	19.2	23.0	23.0	23.0	24.0	.110		0		
277	69	13	9	M	23.8	25.0	24.7	24.3	23.5	.0	.0	.0	.0	8.0	12.0	15.0	17.5	17.5	.0	.0	.0	.0	.100		1		
278	69	18	9	E	.0	15.3	17.6	19.5	19.0	19.3	18.5	20.3	22.0	.0	13.5	17.2	19.0	18.0	18.5	19.0	16.0	17.5	.022		1		.54
279	69	19	9	M	.0	20.8	20.3	20.3	.0	.0	.0	.0	.0	.0	10.0	10.0	14.0	.0	.0	.0	.0	.0	.032		1		
280	69	20	9	E	.0	15.5	18.8	19.8	19.8	19.6	19.5	22.0	24.0	13.5	14.8	16.2	17.0	17.7	20.0	19.0	18.0	18.0	.023		1		.42
281	69	21	9	M	20.7	22.0	22.0	21.8	21.0	20.8	.0	.0	.0	10.0	9.8	10.2	12.0	16.5	19.7	.0	.0	.0	.035		0		
282	69	21	9	E	.0	19.0	21.2	21.6	21.0	20.0	20.0	20.5	.0	12.0	13.6	16.0	17.0	18.0	19.7	20.2	18.5	.0	.060		0		
283	69	22	9	M	.0	22.2	22.4	21.0	.0	.0	.0	.0	.0	.0	8.0	9.0	13.0	.0	.0	.0	.0	.0	.030		0		
284	69	22	9	E	.0	20.3	21.2	22.0	21.0	20.2	20.5	22.0	24.0	12.0	13.3	15.5	16.5	17.7	18.8	19.0	18.8	21.0	.058		0		
285	69	23	9	E	.0	15.7	16.3	18.8	18.6	19.0	18.8	21.0	.0	12.0	14.0	14.7	15.5	16.4	16.8	17.0	17.0	.0	.022		0		
286	69	27	9	E	.0	22.0	23.5	24.0	23.0	.0	.0	.0	.0	12.5	14.8	15.0	18.0	20.0	.0	.0	.0	.0	.155		0		
287	69	28	9	E	.0	21.5	22.0	22.0	22.0	21.0	20.6	21.5	27.0	.0	13.0	13.4	15.0	15.5	17.0	18.2	18.5	19.2	.050		0		
288	69	29	9	M	.0	22.0	23.5	.0	.0	.0	.0	.0	.0	.0	11.0	11.0	.0	.0	.0	.0	.0	.0	.045		0		
289	69	30	9	M	.0	22.0	22.7	20.0	.0	.0	.0	.0	.0	.0	.0	11.0	13.2	.0	.0	.0	.0	.0	.020		1		
290	69	30	9	E	.0	23.0	24.5	24.0	23.0	20.0	19.4	20.8	.0	.0	14.0	13.5	14.0	15.5	18.5	19.2	18.5	.0	.083	18	1	0	
291	69	1	10	E	.0	.0	.0	.0	21.0	20.8	.0	.0	.0	.0	.0	.0	.0	16.5	19.0	.0	.0	.0	.042	15	11	3	
292	69	4	10	E	.0	.0	.0	.0	.0	.0	.0	21.0	.0	.0	.0	.0	.0	.0	.0	17.0	.0	.0	.038	13	0	2	
293	69	6	10	M	18.0	20.0	20.0	21.0	.0	.0	.0	.0	.0	.0	12.0	13.3	14.7	.0	.0	.0	.0	.0	.017	13	0	0	
294	69	9	10	M	18.0	19.0	20.0	20.7	.0	.0	.0	.0	.0	.0	12.0	13.5	16.0	.0	.0	.0	.0	.0	.028	13	0	2	
295	69	9	10	E	18.0	18.2	19.7	20.3	21.0	20.3	.0	21.5	.0	12.0	14.3	15.7	17.0	18.0	18.3	.0	19.6	.0	.020	14	0	3	
296	69	10	10	M	20.0	20.3	21.2	21.0	21.0	20.8	20.3	21.0	.0	.0	11.0	13.3	16.0	19.4	20.4	19.7	19.5	.0	.038	14	0	0	
297	69	10	10	E	23.0	23.2	22.8	22.3	22.0	19.8	20.7	21.8	.0	14.0	14.7	15.5	17.0	18.6	19.3	21.5	21.5	.0	.042	15	0	2	
298	69	12	10	E	.0	25.0	25.5	24.7	23.0	20.5	20.8	21.3	.0	.0	15.5	16.5	18.2	20.0	23.5	22.3	23.0	.0	.150		11		
299	69	15	10	M	17.0	20.3	19.7	19.0	.0	.0	.0	.0	.0	.0	.0	12.0	13.2	.0	.0	.0	.0	.0	.018	14	0	0	
300	69	15	10	E	18.0	17.0	18.0	.0	.0	.0	.0	.0	.0	14.0	16.5	18.5	.0	.0	.0	.0	.0	.0	.020		11		
301	69	16	10	M	20.8	21.5	21.2	21.0	22.0	.0	.0	.0	.0	12.5	11.3	12.5	13.7	17.0	.0	.0	.0	.0	.052	14	0	0	
302	69	18	10	M	22.0	22.1	21.8	21.0	22.0	21.3	.0	.0	.0	12.0	12.8	13.6	16.0	17.0	21.0	.0	.0	.0	.030	14	0	0	
303	69	18	10	E	18.5	20.0	19.7	20.8	21.3	21.7	23.0	24.0	.0	13.0	16.5	17.0	16.5	17.8	17.8	.0	.0	.0	.040	13	1	2	

* Other Parameters:
- B - Atmospheric Turbidity
- TT - Turbidity Type
- CL - Cloud and Snow Cover
- A - Solar Aureole
- LCR - Logarithm of the Color Ratio

Figures 5a and 5b give plots of DA and DB respectively, as a function of atmospheric turbidity for a solar elevation angle of 6 degrees. For brevity, only the results at this solar angle are presented; similar trends in the data were observed at the other solar elevation angles(see Figures 6 and 7). Figure 5a suggests that for turbidity values less than 0.15, DA increases rapidly as turbidity increases and it approaches an asymptotic limit thereafter. For turbidities greater than 0.3, there is some indication that DA decreases, but there are too few data points to substantiate this trend. Figure 5b indicates that DB also increases as a function of turbidity, however, not as much as DA.

4.2 Sea Surface Reflection

For observations of DA made at a lake or sea shore, Fraser[6] showed that a decrease of up to 4 degrees can be explained if Fresnel reflection from the water surface is considered. Furthermore, both observations and theory agree that such effects on DB (in the morning observations), are less likely. Since our data were obtained 10 to 20 km from the Atlantic Ocean, one needed to determine if the same effects could still be observed. Therefore, morning and evening observations of each neutral point were compared because the neutral point-ocean-sun geometry is (for most of the year), different at these times. To avoid any confusion with volcanic effects, only the data prior to 1982 was con-

6. Fraser, R.S. (1968) Atmospheric neutral points over water, J. Opt. Soc. Am. 58:1029-1031.

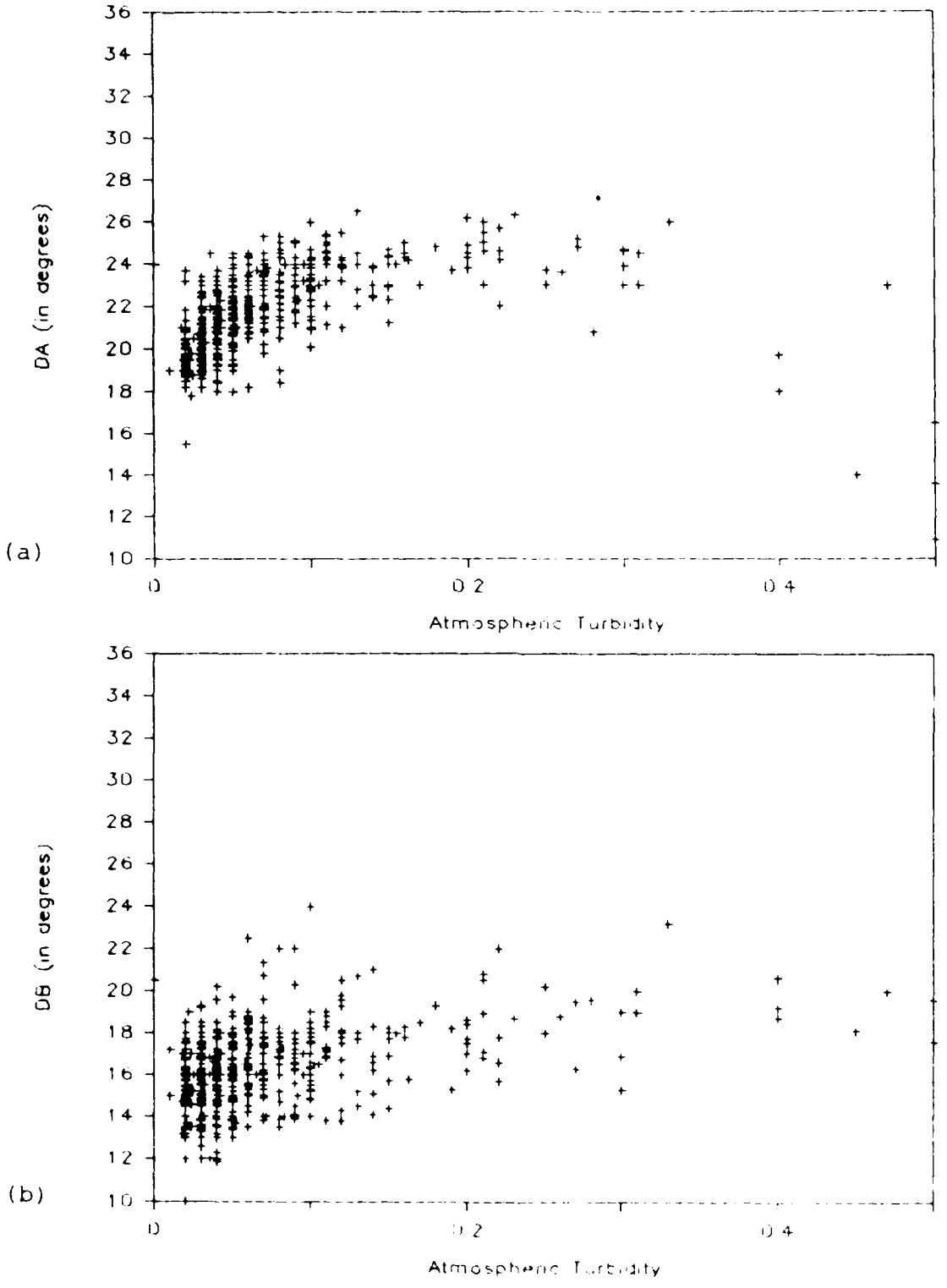

Figure 5. Values of (a) DA and (b) DB as a Function of Atmospheric Turbidity for the Time Period 1968 to 1977. These Data Are for a Solar Elevation Angle of 6 Degrees

sidered. Furthermore, those records of data having turbidities greater than 0.3 or cirrus clouds present at the time of observation were not included.

Figures 6a and 6b separate DA and DB according to morning and evening observations for a solar elevation angle of 14 degrees. Figure 6a indicates that are no systematic differences in DA for the two times of observation. The same analysis was performed for the other positive solar elevation angles and no distinct differences were observed. In light of this, it was felt that the Atlantic was too far away to affect evening observations of DA and, therefore, no corrections for it were necessary.

Interestingly, Figure 6b suggests that our morning observations of DB may be lower than those taken in the evening. These differences however, are too small to be of importance and therefore, morning and evening observations of DB will not be treated differently in the remainder of this report.

4.3 Snow Cover

An analysis similar to that in Section 4.2 was performed for snow-covered and bare-ground conditions. This was deemed necessary because the amount of sunlight reflected by a snow-covered surface is substantial, especially when compared with a vegetative one. Previous work by Neuberger[7]

7. Neuberger, H. (1941) The influence of the snow cover on the position of Arago's neutral point, Bull. Am. Meteorol. Soc. 22:348-351.

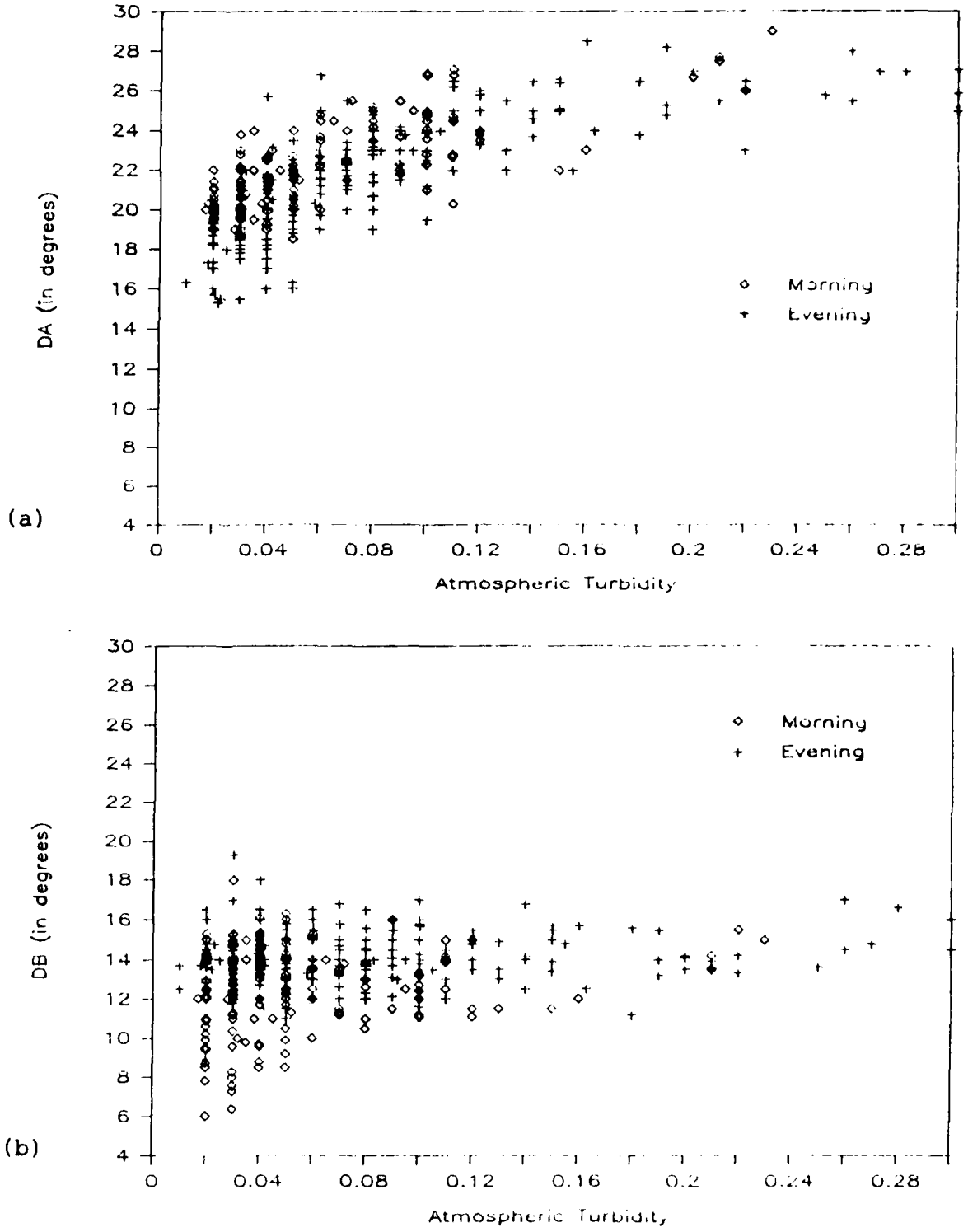

Figure 6. Morning and Evening Values of (a) DA and (b) DB as a Function of Atmospheric Turbidity for the Time Period 1968 to 1977. These Data Are for a Solar Elevation Angle of 14 Degrees

suggests that DA may be lowered by about 2 degrees over snow-covered fields due to the increased multiple scattering.

In Figures 7a and 7b, DA and DB at a solar elevation of 20 degrees are separated according to snow and non-snow surface conditions. No systematic differences occured between the two types of surface conditions. Similar conclusions have been made by Chandrasekhar[3]. His calculations showed that the position of a neutral point is relatively insensitive to ground albedo.

5. TURBIDITY CORRECTIONS APPLIED TO THE NEUTRAL POINT DATA

The previous chapter showed that neutral points are not influenced by the characteristics of the ground, only the state of the atmosphere itself. That is, most of the scatter often observed in the neutral point data can be attributed to daily variations in tropospheric turbidity. It seems reasonable to try to compensate or correct for these day-to-day variations because they may overshadow any movement in the points caused by the presence volcanic aerosols. This section describes the methods used to compensate for tropospheric effects during nonvolcanic and volcanic periods. Volz then discusses his examination of the turbidity-corrected data.

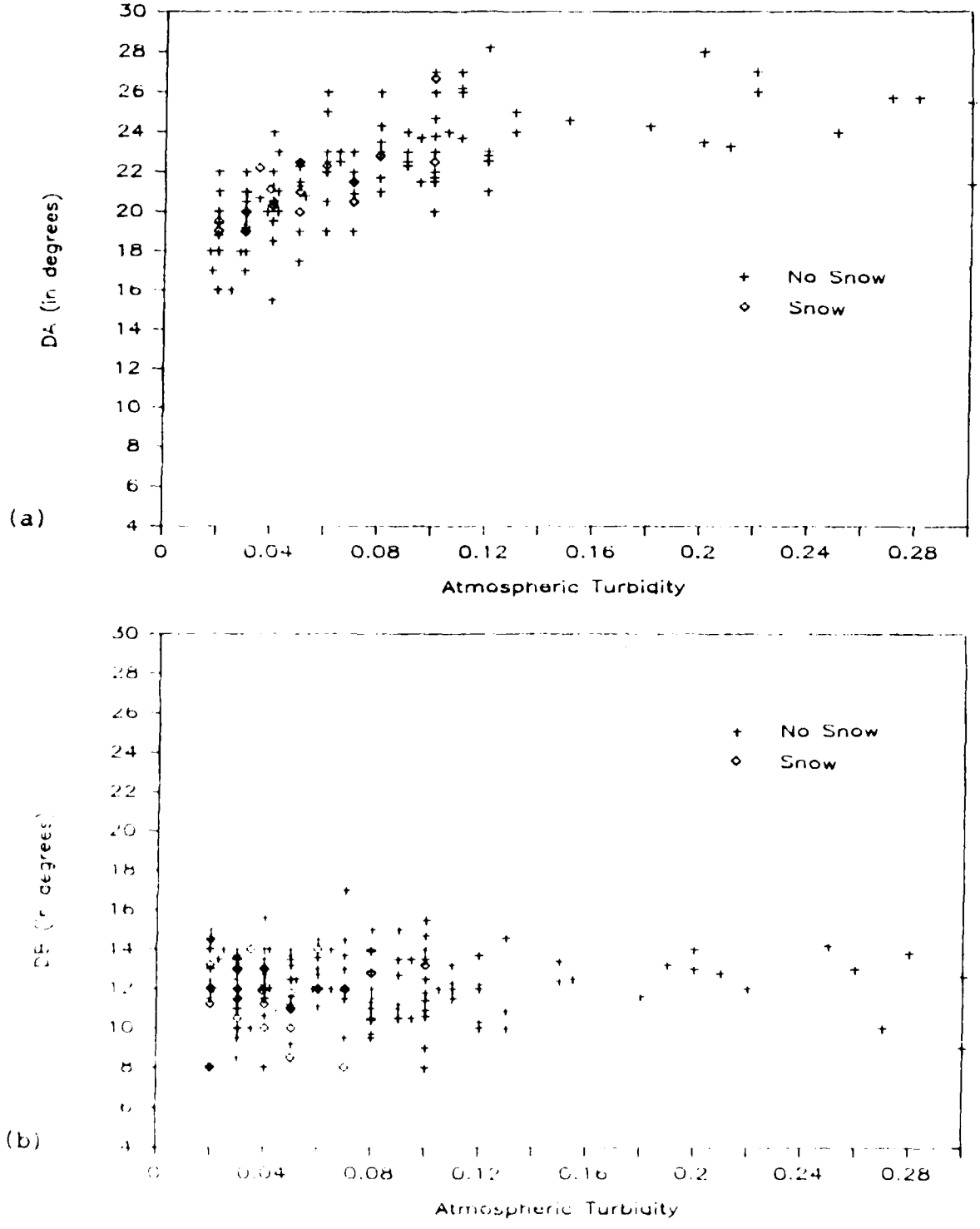

Figure 7. Values of (a) DA and (b) DB as a Function of Atmospheric Turbidity for Bare and Snow-Covered Ground Conditions from 1968 to 1977. These Data Are for a Solar Elevation Angle of 20 Degrees

5.1 Nonvolcanic Periods

Using Figures 5a, 5b and similar plots for the other fixed solar elevation angles, the first step in the correction scheme was to draw best-fit curves through the data, and to record the values for DA and DB corresponding to a turbidity of 0.05. Deviations of DA and DB from the values at a B equal to 0.05 were then estimated for predetermined values of B by subtracting the value for DA and DB along the curve from the value measured at 0.05. As an example, Figure 8 illustrates how the correction, Δ DA, is derived for an atmospheric turbidity of 0.2 (see Tables 3 and 4 for the complete set of corrections for DA and DB). The corrections were then applied to the neutral point data prior to the El Chichon eruption and after May 1983. This was done by matching the observed atmospheric turbidity for a given set of data with the turbidity values in Tables 3 and 4, and by applying the corresponding correction values. Whenever an observed turbidity value fell between two of the turbidities in Tables 3 and 4, the correction was obtained by means of a linear interpolation between the corrections associated with the two turbidities.

With the corrections described above, the neutral point data are normalized in effect, to an atmosphere with 0.05 turbidity. This value of turbidity was chosen because the majority of the points are clustered around it. The approach does not take into account other effects caused by the other parameters in the database and therefore, should be treated

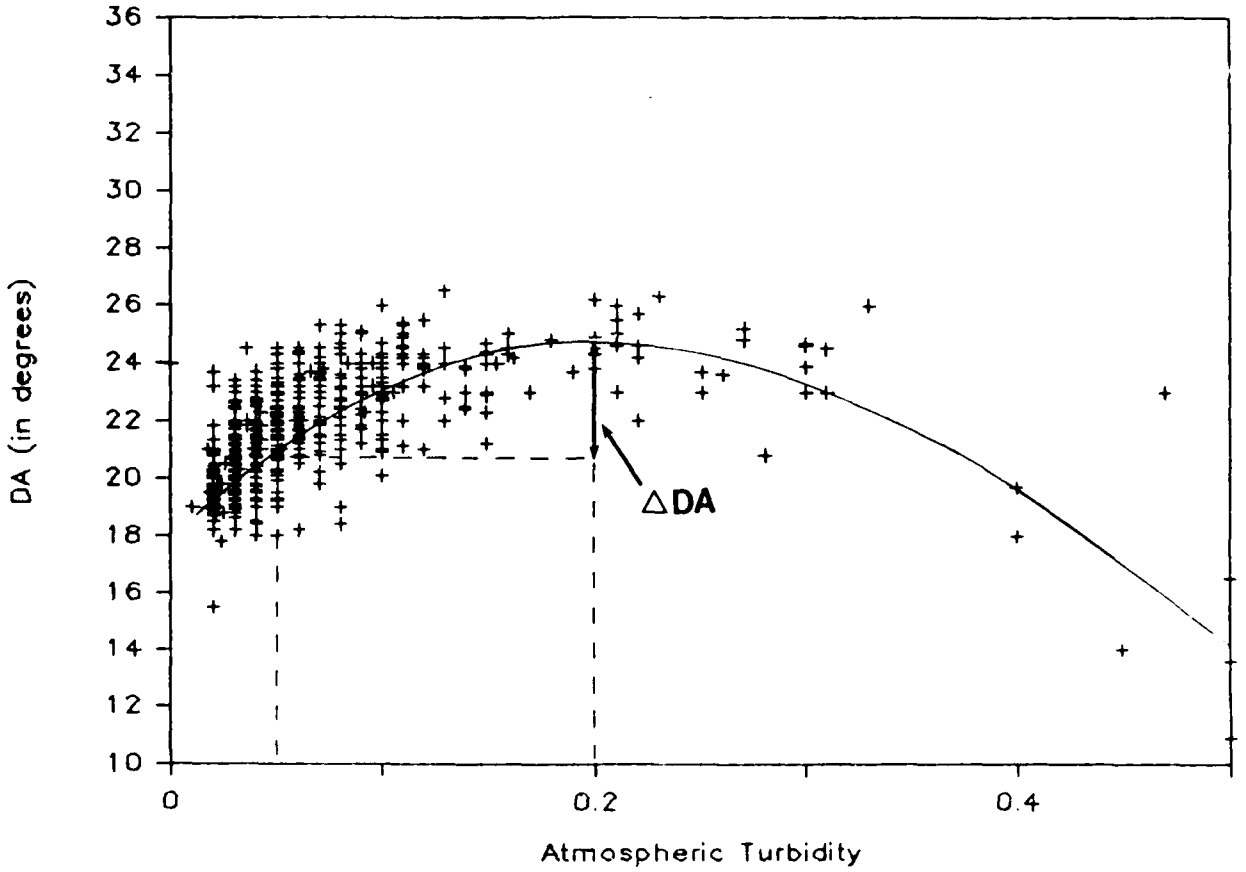

Figure 8. The Method of Correcting the Neutral Point Data for Atmospheric Turbidity. In This Example, for H Equal to 6 Degrees, the ΔDA is -4.0 Degrees for an Atmospheric Turbidity of 0.2

Table 3. Tropospheric Aerosol Corrections, in Degrees, for DA at Fixed Values of Atmospheric Turbidity and Solar Elevation Angle

Solar Elevation Angle (Degrees)	Fixed Values of Turbidity							
	0.55	0.35	0.20	0.10	0.05	0.02	0.01	0.0
20	-3.0	-3.0	-4.0	-2.4	0.0	2.2	4.5	4.5
14	2.0	-3.0	-5.0	-2.3	0.0	2.7	5.0	5.0
10	4.0	-3.0	-5.0	-2.8	0.0	2.4	4.4	4.5
6	8.0	-2.0	-3.5	-2.0	0.0	1.6	3.3	3.3
3	8.0	1.0	-2.0	-1.15	0.0	1.1	2.8	2.8
0	6.0	0.0	-2.0	-1.1	0.0	0.8	2.3	2.3
-2	7.0	1.0	-0.5	-1.05	0.0	-0.1	1.6	1.6
-4	8.0	4.0	0.0	-0.85	0.0	0.45	2.5	2.5
-6	8.0	4.0	-2.0	-0.95	0.0	2.0	2.7	2.7

Table 4. Tropospheric Aerosol Corrections, in Degrees, for DB at Fixed Values of Atmospheric Turbidity and Solar Elevation Angle

Solar Elevation Angle (Degrees)	Fixed Values of Turbidity							
	0.55	0.35	0.20	0.10	0.05	0.02	0.01	0.0
20	-5.0	-1.0	0.0	-0.35	0.0	0.0	0.0	0.0
14	-4.0	-3.0	-2.0	-0.7	0.0	0.25	0.23	0.23
10	-3.5	-3.0	-2.0	-0.6	0.0	0.1	0.75	0.75
6	-2.5	-3.0	-2.0	-1.5	0.0	0.85	1.2	1.2
3	-2.0	-2.0	-2.0	-1.1	0.0	0.75	1.2	1.2
0	0.0	-2.0	-2.0	-1.9	0.0	0.95	1.8	1.8
-2	2.0	-2.0	-3.0	-2.0	0.0	1.1	1.6	1.6
-4	2.0	-2.0	-3.0	-2.0	0.0	1.4	1.7	1.7
-6	2.0	2.0	-3.0	-2.0	0.0	1.2	1.0	1.0

as a first approximation. Furthermore, the scheme assumes that the contribution to atmospheric turbidity from the stratospheric aerosols is negligible, or at least constant with time. This is probably true for nonvolcanic periods but not for highly volcanic periods such as the months following the El Chichon eruption.

5.2 Volcanic Periods

To determine to what extent volcanic dust in the stratosphere affects the values of atmospheric turbidity, Volz[8] provided the monthly averages of atmospheric turbidity for the period prior to the El Chichon eruption and the monthly averages beginning in August 1982 (see Table 5). It is clear from these data that the El Chichon dust cloud caused the atmospheric turbidity to increase substantially during the period from October 1982 to May 1983. Using measurements of peak optical depths, McCormick et al.[9] have monitored the northward movement of the El Chichon cloud. Their results confirm the presence of the El Chichon dust cloud over northern midlatitudes during the same time period.

8. Volz, F.E. (1984) Volcanic turbidity, skylight scattering functions, and sky polarization and twilight in New England during 1983, Appl. Opt. 23: 2589-2593.
9. McCormick, M.P., Swissler, T.J., Fuller, W., Hunt H., and Osborn, M.T. (1984) Airborne and ground-based lidar measurements of the El Chichon stratospheric aerosol from 90 degrees N to 56 degrees S, Geof. Int. 23:187-221.

Table 5. Monthly Averages of Turbidity at Lexington, Massachusetts for the Years 1980 to 1983.

Month	Year 1980 - 1981	1982	1983
January	0.04	0.075	0.11
February	0.06	0.08	0.12
March	0.065	0.08	0.125
April	0.075	0.095	0.20
May	0.13	0.13	0.17
June	0.16	0.17	0.12
July	0.18	0.20	0.11
August	0.14	0.13	0.10
September	0.13	0.135	0.11
October	0.08	0.09	0.05
November	0.06	0.10	0.04
December	0.05	0.12	0.05

Based on the large increases of B, it is inappropriate to apply the correction described in Section 5.1 to the data taken between October 1982 and May 1983. In effect, one would be overcompensating for the movement of the neutral points because the corrections in Section 5.1 are for tropospheric aerosols only. Therefore, the correction scheme was modified before applying it to data taken during the El Chichon volcanic period.

Except for one additional step, the method used to compensate for tropospheric effects during the El Chichon volcanic period was the same as that for nonvolcanic periods. Specifically, first the tropospheric turbidity associated with a given set of observations was isolated by subtracting a turbidity value representative of the El Chichon cloud. That is,

$$B_{trop} = B - B_v',$$

where B_{trop} is the tropospheric turbidity and B_v' is the turbidity of the volcanic dust cloud. Using B_{trop} in place of B, the volcanic data was then corrected using the method described in Section 5.1 and the set of corrections in Tables 3 and 4.

Monthly values for B_v' were obtained by subtracting the average values of turbidity for each month of the El Chichon volcanic period ($\overline{B_v}$) from the average values for the same

months during 1980 and 1981 ($\overline{B_{nonv}}$). That is,

$$B_v' = \overline{B_v} - \overline{B_{nonv}}$$

for each month. Here it should be noted that the day-to-day variations in the El Chichon cloud are assumed to be relatively small. This seems reasonable because the cloud was well mixed by the time it reached the latitude of the observations and therefore, any changes in the turbidity of the cloud should be slowly varying with time. The monthly values of B_v' are given in Table 6.

Table 6. Monthly Values of the Turbidity of the El Chichon Dust Cloud (B_v'), from Measurements at Bedford and Lexington, Massachusetts

1982			1983				
Oct.	Nov.	Dec.	Jan.	Feb.	Mar.	Apr.	May
0.01	0.04	0.07	0.07	0.06	0.06	0.12	0.04

5.3 Examination of the Corrected Data

With the average turbidity effects removed, plots in the form of Figures 2 and 3 were prepared for all the neutral point data. Many probable defects were noted, especially by looking at the deviations from the seasonal trend of DBA. In most cases, Volz could determine the source of the error and the data were edited accordingly. A number

of errors also arose from wrong turbidity values and from incorrect classification as not being cirrus-veil cases.

The complete database has not been included as a part of this report because it is too extensive. Copies of the turbidity-corrected data can be obtained from Volz at AFGL. The turbidities reported with the turbidity-corrected data already have the monthly values of B_v' subtracted. If a turbidity equaled zero after subtracting B_v', that turbidity has been given a value of 0.02.

6. PRESENTATION OF THE DATA BY GROUP AVERAGES

In Chapter 4 it was shown that the neutral points were not affected by the characteristics of the ground, only by the state of the atmosphere. As a result, Chapter 5 was an attempt to eliminate the movement in the neutral points caused by tropospheric aerosols.

The corrected neutral point data is now presented in a manner that reveals their behavior during various stratospheric phenomena. Specifically, the stratospheric aerosol number densities and observed twilight color ratios will be used as guides to separate the data into groups that coincide with the time periods of known volcanic influences (minor and major) and seasonal events. In effect, the grouping of sets of observations allows the entire data set to be presented in a compact form and still resolve any movement in the neutral points caused by a change in the stratospheric aerosol.

6.1 Grouping

The grouping of the data was based primarly on stratospheric aerosol data, but measurements of the twilight color ratios (CR) were considered because they contain details that may help explain the behavior of the neutral points. Figure 9 is a comparision between the CR measurements by Volz at Bedford, Massachusetts and the stratospheric aerosol concentrations measured with a balloon-borne dustsonde by Hoffman and Rosen[10]. The stratospheric aerosol measurements were taken every four to five weeks near Laramie, Wyoming (42N) and have fluctuations of 5 to 20%. Figure 9 indicates that the CR measurements follow the same trends as the Hoffman and Rosen data, but the CR are always lower during spring and summer than in the fall and winter. The lower values of CR may be due to the higher turbidity near the tropopause during the spring and summer. Therefore, in addition to the nonvolcanic, moderate and strong volcanic periods, groups of spring/summer and fall/winter CR conditions were distinguished in the graphs and in the numerical evaluation. Details on the 40 groups selected are given in Table 7. Unfortunately, the detailed trend of CR during the El Chichon period was not available at the time Table 7 was prepared and therefore, the grouping of data in the El Chichon period was not optimal.

The average values and standard deviations of DA and DB and average values of DBA were then calculated for each

10. Hoffman, D., and Rosen, J. (1986) Atmospheric effects, SEAN Bull. 11:No.5, 20.

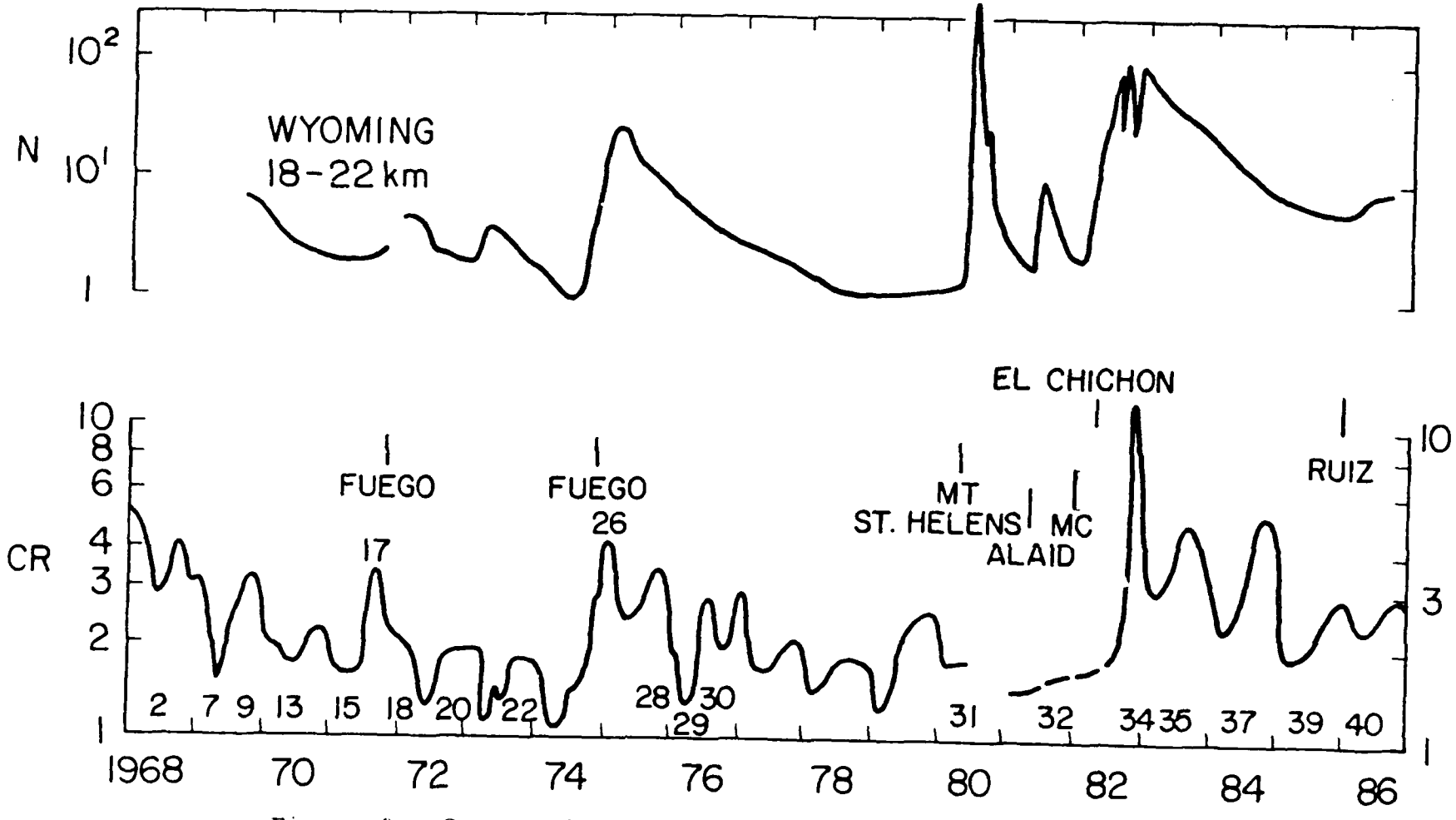

Figure 9. Stratospheric Aerosol Number Density (N), in Particles (with Radii Greater Than 0.24 Microns) per Milliliter, and the Trends of Peak Color Ratio over 2 to 4 Week Periods for the Years 1968 to 1986. The Numbers Above the Time Axis Correspond to the Groups in Table 7. Volcanic event MC refers to the so called Mystery Cloud which probably was caused by a volcano in the tropics.

Table 7. The Grouping of the Neutral Point Data

Group Number	Time Period		Record Numbers	Classification*	Comments
	Start Date	End Date			
1	4/12/68	6/20/68	13-23	WV	Still Remnants of Volcanic Aerosols from Several Tropical Eruptions between 1962 and 1966
2	6/21/68	7/31/68	24-34	WV-S	-
3	8/11/68	9/28/68	35-64	WV	-
4	10/1/68	10/31/68	65-95	WV	-
5	1/11/68	12/1/69	96-154	WV	Slightly Lower CR Than in Previous Period
6	1/15/69	2/16/69	155-179	WV-S	Start of Spring Effect
7	3/4/68	4/30/68	180-214	WV-S	-
8	5/1/68	6/30/68	215-246	WV	Rising CR
9	7/19/69	9/30/69	247-290	WV	High Level of CR
10	10/1/69	11/21/69	291-316	WV	Local Peak of CR
11	12/4/69	1/31/70	317-367	-	Sudden Drop of Volcanic CR
12	2/13/70	3/30/70	368-405	(NV-S)	Stable and Low CR
13	4/3/70	7/9/70	406-440	NV-S	Typical Spring/Summer Minimum
14	8/4/70	1/23/71	441-511	NV-F	Higher CR
15	2/1/71	7/3/71	512-552	NV-S	Sudden Drop of CR
16	8/5/71	9/26/71	553-571	-	Higher and Fluctuating CR
17	10/1/71	1/3/72	572-609	WV	Sudden Arrival of Fuego Aerosol and Strong Twilight Colors; Eruption Was on 9/14/71 in Guatemala
18	2/1/72	2/16/72	610-623	(WV)	End Phase of Fuego Twilights
19	2/22/72	7/30/72	624-643	NV-S	Spring-Summer Minimum of CR
20	8/4/72	1/30/73	644-714	NV-F	Higher CR (After a Few May and June Observations)
21	2/4/73	8/16/73	715-755	NV-S	-
22	9/10/73	2/24/74	756-820	NV-F	-
23	3/7/74	6/14/74	821-839	NV-S	Very Low CR
24	7/6/74	11/10/74	840-871	NV-F	Rising CR, Possibly from Fuego Eruptions of 10/74
25	11/27/74	12/18/74	872-881	(WV)	Definite Arrival of Fuego Aerosol

Table 7. (cont.)

Group Number	Time Period		Record Numbers	Classification*	Comments
	Start Date	End Date			
26	12/26/74	2/26/75	882-898	WV	Bulk of Fuego Aerosol
27	3/3/75	9/29/75	899-918	WV-S	Weak Spring/Summer Minimum of CR
28	10/7/75	1/6/76	919-926	(WV)	High CR
29	1/10/76	7/25/76	927-937	NV-S	Decrease of CR
30	9/6/76	3/11/77	938-959	NV-F	Higher CR
	THREE YEAR GAP IN DATA				
31	5/22/80	5/28/80	960-964	NV-F	Mt. St. Helens Eruptions On and After 5/18/80; No Enhanced Twilights Observed in Bedford, MA
32	10/31/81	10/2/82	965-995	WV	After the Eruption of El Chichon from 4/3/82 to 4/4/82 in Mexico, the Increase in Twilight Effects Were Probably Due to the Volcanic Aerosol Arriving in the Lower Stratosphere
33	10/10/82	11/27/82	996-1019	V	Still Increasing Twilight Effects; Measurable Turbidity Increases and Significant Changes in Neutral Points, First in DB
34	12/4/82	3/26/83	1020-1056	V	Bulk of the El Chichon Aerosol; Some Twilight Displays Indicate That the Dust Layer Is Very High in the Stratosphere, Possibly in Relation to the Recovering of DB from 1 to 3 Degrees Solar Depression Angle.
35	4/23/83	8/25/83	1057-1099	(V-S)	Slowly Declining Volcanic Effects and Lower CR
36	9/1/83	2/27/84	1100-1140	MV	Slowly Declining Volcanic Effects
37	3/1/84	7/25/84	1141-1177	MV-S	Further Declining Volcanic Effects
38	8/8/84	1/29/85	1178-1239	(MV)	Last Traces of the Scattering by the El Chichon Aerosol Disappear from the Daytime Sky
39	2/10/85	11/23/85	1240-1295	WV-S	Neutral Points Nearly Normal
40	12/2/85	6/17/86	1296-1357	(WV)	Neutral Points Normal

* Classification:
V - Strong Volcanic Period and Neutral Points Strongly Affected
MV - Moderate Volcanic Period and Neutral Points Barely Affected
WV - Weak Volcanic Period and No Effect on Neutral Points
NV - Nonvolcanic Period
-S - Spring/Summer Minimum of CR
-F - Fall/Winter Maximum of CR
( ) - Weak Effects

of the groups in Table 7 (see Tables 8, 9 and 10). When computing the averages, data having a turbidity greater than 0.30 or cirrus clouds present at the time of observation were not included. Furthermore, some groups did not have data at 20 and -6 degrees solar elevation angle and therefore, values had to be estimated. These values are denoted in brackets.

6.2 3-D Plots and Staggered Plots

Figures 10, 11 and 12 are 3-D plots of DA, DB and DBA respectively, as a function of solar elevation angle and group number. The vertical axes have been chosen so that DA, DB and DBA all have the same scale. Note that the plotting package has assigned equally spaced intervals between the nine fixed solar elevation angles and, therefore, the data at the far left has been compressed. Also, the perspective of the 3-D plots causes the El Chichon peak to hide most of the later profiles. By reversing the sequence of groups 32 to 40, the slow decline of DB is shown in Figure 13.

Staggered plots of DA, DB and DBA are given in Figures 14a, 14b and 14c for the 40 groups. The standard deviations of DA and DB have been plotted as vertical bars in Figures 14a, 14b and 14c. In contrast to the 3-D plots, the staggered plots have solar elevation angle plotted with proper spacing between the nine fixed solar elevation angles.

Table 8. Averaged Values of DA and Their Standard Deviations (In Parenthesis) for the Groups in Table 7. The Brackets Indicate Those Values That Have Been Estimated. Also, a Standard Deviation of 0.0 Means That Only One Observation Was Available

Group Number	Solar Elevation Angle (Degrees)								
	20	14	10	6	3	0	-2	-4	-6
1	21.1 (0.0)	21.4 (1.7)	21.0 (1.3)	21.8 (1.2)	22.9 (1.0)	21.9 (0.7)	20.1 (1.4)	20.1 (0.4)	21.4 (2.7)
2	[21.3]	21.8 (0.4)	20.7 (0.4)	21.7 (0.9)	21.2 (1.0)	20.4 (0.6)	20.0 (0.4)	20.0 (1.4)	22.5 (0.9)
3	21.3 (1.4)	23.2 (1.1)	22.7 (1.5)	22.2 (1.3)	21.8 (1.2)	20.9 (1.1)	21.0 (1.1)	21.7 (2.0)	25.3 (2.1)
4	23.8 (1.3)	24.0 (1.5)	23.5 (1.3)	23.0 (1.3)	23.1 (1.4)	22.1 (1.3)	22.9 (2.0)	23.3 (2.1)	28.2 (2.3)
5	20.9 (0.2)	21.5 (1.1)	22.1 (0.9)	22.1 (1.0)	21.5 (0.9)	20.7 (0.9)	20.7 (1.6)	20.2 (1.4)	23.9 (3.7)
6	21.1 (0.9)	21.3 (1.2)	21.4 (1.0)	21.5 (1.2)	20.4 (1.1)	19.3 (0.7)	18.4 (0.7)	18.9 (0.8)	21.7 (0.9)
7	20.2 (1.3)	21.4 (1.0)	21.2 (1.0)	21.5 (0.9)	21.0 (0.9)	19.8 (1.0)	18.9 (1.0)	19.3 (1.1)	22.2 (2.8)
8	20.6 (1.7)	21.5 (1.6)	22.2 (1.5)	22.1 (1.7)	21.7 (1.3)	19.9 (1.7)	19.5 (1.2)	20.0 (1.1)	22.8 (2.6)
9	21.5 (1.4)	21.5 (1.9)	21.4 (1.9)	21.6 (1.1)	20.7 (1.3)	19.9 (0.8)	19.5 (0.8)	21.1 (0.9)	24.1 (2.2)
10	21.0 (1.4)	22.3 (1.2)	22.4 (1.2)	21.9 (0.7)	21.7 (0.6)	20.7 (1.0)	20.6 (1.0)	21.7 (0.9)	24.0 (0.0)
11	21.5 (1.3)	22.2 (1.4)	22.0 (1.1)	21.9 (1.0)	21.2 (0.9)	20.2 (0.9)	19.5 (0.9)	20.8 (1.0)	25.9 (1.6)
12	22.4 (0.9)	21.8 (0.9)	22.0 (0.8)	21.9 (0.6)	21.1 (0.7)	19.8 (0.7)	19.3 (0.7)	20.6 (0.6)	24.2 (0.4)
13	18.7 (2.6)	20.9 (2.1)	20.9 (1.5)	21.2 (0.7)	20.8 (0.6)	19.5 (1.1)	18.8 (1.5)	19.9 (1.7)	26.4 (1.7)
14	20.6 (1.6)	20.9 (2.1)	20.8 (1.8)	20.2 (1.5)	20.0 (1.3)	18.9 (1.3)	18.7 (1.2)	20.4 (1.0)	25.0 (1.8)
15	20.9 (0.8)	20.0 (1.9)	21.8 (0.9)	21.0 (0.8)	20.2 (1.2)	19.6 (1.1)	19.1 (0.6)	19.5 (0.7)	24.1 (0.8)
16	23.2 (0.9)	22.0 (0.9)	21.9 (0.9)	21.8 (0.6)	21.0 (0.9)	19.2 (0.5)	19.0 (0.6)	19.7 (0.8)	24.5 (1.1)
17	22.5 (0.0)	21.9 (1.8)	20.8 (1.6)	20.4 (1.2)	20.2 (1.2)	19.4 (0.9)	19.0 (0.8)	21.4 (1.0)	26.0 (1.5)
18	22.1 (0.6)	22.8 (0.9)	22.1 (0.6)	21.3 (1.5)	21.0 (0.6)	19.8 (0.8)	19.6 (0.7)	21.4 (0.8)	23.7 (0.0)
19	[21.8]	21.8 (0.0)	21.6 (2.0)	21.6 (1.1)	21.4 (0.8)	17.9 (0.8)	18.6 (0.6)	20.2 (1.5)	[25.0]
20	22.6 (1.6)	21.9 (1.1)	21.4 (1.1)	20.9 (0.9)	20.1 (1.0)	19.0 (0.9)	18.8 (1.0)	20.9 (1.3)	24.0 (6.4)

Table 8. (cont.)

Group Number	Solar Elevation Angle (Degrees)								
	20	14	10	6	3	0	-2	-4	-6
21	21.8 (2.4)	21.6 (1.9)	21.2 (1.6)	21.1 (0.9)	20.5 (0.9)	19.0 (0.9)	18.6 (0.8)	20.3 (1.1)	24.6 (2.6)
22	21.4 (0.7)	21.7 (1.6)	20.0 (1.5)	20.0 (0.9)	20.0 (0.8)	19.0 (0.7)	18.7 (0.9)	21.0 (1.1)	25.4 (2.1)
23	[21.2]	21.3 (1.2)	20.9 (0.8)	20.5 (0.8)	19.7 (0.7)	18.6 (0.5)	18.3 (0.9)	20.2 (1.2)	24.7 (2.3)
24	20.2 (0.0)	20.3 (1.2)	20.9 (1.0)	20.5 (0.7)	20.0 (0.9)	19.1 (1.1)	18.6 (1.0)	21.2 (1.2)	28.2 (2.5)
25	[23.0]	24.0 (0.0)	22.2 (1.7)	22.5 (1.2)	21.8 (1.1)	20.7 (1.2)	20.5 (1.4)	21.4 (1.3)	26.3 (2.3)
26	20.3 (0.8)	22.3 (0.5)	21.9 (1.5)	22.3 (1.1)	22.3 (0.8)	21.6 (1.3)	20.5 (1.0)	21.0 (1.4)	25.2 (2.3)
27	[21.5]	21.6 (2.5)	22.4 (1.0)	22.5 (0.9)	22.2 (1.0)	20.9 (1.2)	20.2 (1.1)	20.8 (0.8)	22.3 (2.8)
28	[22.3]	22.5 (0.0)	22.1 (1.4)	21.6 (1.1)	20.8 (0.7)	20.1 (0.8)	19.3 (0.7)	21.6 (0.4)	25.5 (1.5)
29	[21.5]	20.8 (0.0)	20.5 (1.9)	21.1 (0.8)	20.4 (0.8)	19.5 (1.1)	19.2 (1.0)	21.2 (2.3)	25.1 (1.6)
30	20.5 (0.0)	21.3 (0.6)	21.3 (0.9)	21.2 (1.5)	20.9 (1.0)	19.7 (0.8)	19.8 (0.6)	21.5 (1.2)	27.2 (1.3)
31	22.0 (0.0)	22.0 (0.0)	21.7 (0.7)	21.7 (0.8)	20.3 (1.0)	19.1 (1.1)	17.8 (0.8)	20.6 (1.8)	23.0 (0.0)
32	22.2 (1.5)	22.1 (1.1)	22.0 (1.1)	21.8 (1.2)	21.7 (1.8)	20.8 (1.4)	19.8 (1.5)	21.6 (1.4)	25.5 (2.9)
33	26.6 (1.4)	27.2 (2.5)	25.8 (3.5)	26.7 (3.1)	26.5 (2.8)	24.7 (2.6)	21.8 (1.7)	22.8 (2.5)	24.7 (3.9)
34	29.5 (1.6)	30.9 (2.2)	31.5 (2.3)	31.7 (1.6)	31.6 (1.5)	26.4 (2.2)	20.8 (2.4)	21.6 (2.0)	26.0 (2.9)
35	25.8 (3.7)	24.7 (1.9)	25.5 (2.0)	26.6 (1.5)	27.4 (1.5)	24.6 (1.0)	21.7 (2.1)	22.0 (1.6)	24.6 (2.6)
36	22.8 (1.7)	23.9 (1.5)	24.9 (1.6)	25.7 (1.4)	26.0 (1.2)	24.2 (1.2)	22.3 (1.4)	22.4 (1.4)	23.9 (2.6)
37	22.8 (1.9)	23.1 (1.3)	24.1 (1.2)	25.0 (1.3)	25.5 (1.5)	23.9 (1.2)	21.1 (1.1)	21.9 (1.2)	25.2 (1.0)
38	23.1 (1.6)	23.9 (1.3)	23.9 (1.5)	23.6 (1.1)	23.7 (1.2)	23.1 (1.2)	22.4 (1.5)	23.2 (1.5)	25.9 (2.3)
39	22.2 (1.4)	22.2 (1.3)	22.2 (1.2)	22.2 (1.1)	22.3 (1.4)	22.3 (1.6)	21.2 (1.1)	21.5 (1.2)	25.4 (1.3)
40	22.6 (1.1)	22.8 (1.1)	23.0 (1.1)	23.1 (1.2)	22.5 (1.2)	21.8 (1.0)	21.2 (1.0)	22.5 (1.5)	27.8 (2.4)

Table 9. Averaged Values of DB and Their Standard Deviations (In Parenthesis) for the Groups in Table 7. The Brackets Indicate Those Values That Have Been Estimated. Also, a Standard Deviation of 0.0 Means That Only One Observation Was Available

Group Number	Solar Elevation Angle (Degrees)								
	20	14	10	6	3	0	-2	-4	-6
1	16.9 (0.0)	15.4 (0.0)	16.2 (1.7)	21.1 (1.2)	23.9 (0.7)	25.3 (1.7)	24.8 (0.1)	23.0 (0.6)	23.4 (2.2)
2	14.7 (0.0)	14.6 (0.8)	15.1 (0.9)	16.7 (1.1)	20.2 (1.9)	19.7 (1.6)	20.9 (1.7)	20.7 (1.3)	22.7 (0.8)
3	12.9 (1.2)	13.1 (1.6)	14.7 (1.2)	16.8 (1.2)	18.7 (1.2)	20.3 (1.1)	20.2 (1.0)	19.8 (1.3)	21.6 (2.3)
4	12.6 (1.2)	14.6 (1.5)	16.1 (1.8)	18.2 (1.2)	20.1 (1.5)	21.6 (1.5)	21.7 (1.4)	21.4 (2.2)	22.3 (2.3)
5	11.5 (1.3)	14.6 (1.6)	15.6 (1.5)	17.1 (1.2)	18.5 (1.2)	19.7 (1.3)	19.8 (1.5)	19.4 (1.2)	20.3 (1.4)
6	12.6 (0.8)	14.1 (2.1)	15.1 (1.5)	17.3 (1.1)	18.6 (1.0)	19.5 (0.9)	19.3 (1.2)	18.4 (1.8)	18.7 (1.8)
7	11.9 (2.0)	13.9 (1.5)	15.1 (1.6)	16.4 (1.1)	17.7 (1.1)	19.0 (1.3)	18.5 (1.1)	17.8 (1.3)	15.9 (1.3)
8	12.6 (1.8)	13.0 (1.7)	15.0 (1.9)	16.2 (1.6)	17.4 (1.8)	18.6 (1.7)	18.2 (1.7)	17.9 (1.5)	18.7 (1.8)
9	11.7 (1.6)	12.3 (2.1)	13.8 (2.3)	15.4 (1.9)	17.1 (1.2)	18.6 (1.4)	19.0 (1.0)	18.5 (1.1)	20.1 (1.2)
10	12.4 (1.3)	13.2 (1.8)	14.5 (1.7)	16.1 (1.0)	18.0 (0.9)	19.4 (1.2)	19.6 (1.4)	20.4 (1.6)	19.2 (0.0)
11	12.7 (1.3)	14.2 (1.0)	15.5 (1.4)	16.7 (1.3)	18.1 (1.2)	19.1 (1.3)	19.3 (1.5)	19.0 (1.3)	20.8 (1.9)
12	12.7 (1.5)	13.2 (1.5)	14.9 (1.3)	16.6 (1.1)	17.5 (1.1)	18.2 (1.3)	18.3 (1.2)	18.3 (1.3)	20.5 (0.2)
13	12.8 (0.8)	13.1 (1.3)	14.6 (1.4)	15.5 (1.5)	16.7 (1.5)	17.3 (0.8)	17.3 (1.2)	16.9 (0.8)	20.0 (0.0)
14	12.0 (1.3)	12.5 (1.7)	14.1 (1.6)	15.7 (1.5)	16.2 (1.1)	17.0 (1.1)	16.8 (1.1)	16.9 (1.6)	18.3 (1.6)
15	11.6 (0.9)	12.9 (1.6)	14.4 (1.3)	15.2 (1.6)	16.3 (1.5)	16.9 (0.9)	17.2 (1.1)	17.0 (0.9)	18.0 (0.9)
16	11.9 (0.6)	12.7 (2.0)	13.5 (2.1)	15.7 (1.1)	16.9 (1.2)	17.5 (1.1)	17.5 (1.4)	17.7 (1.2)	17.8 (0.8)
17	10.0 (0.0)	12.8 (1.7)	13.4 (1.6)	15.4 (1.5)	16.2 (1.2)	16.8 (1.1)	17.0 (1.5)	16.8 (1.7)	21.1 (2.3)
18	11.5 (0.0)	13.0 (1.5)	13.8 (1.2)	15.2 (1.4)	16.6 (0.9)	16.8 (0.8)	17.2 (0.7)	16.7 (1.4)	16.4 (0.0)
19	[11.5]	12.6 (1.1)	14.3 (1.1)	14.5 (0.2)	15.1 (1.7)	15.7 (1.6)	16.2 (1.6)	16.5 (0.2)	[17.0]
20	11.6 (1.8)	13.0 (2.0)	14.0 (1.6)	15.3 (1.2)	16.3 (0.9)	17.0 (0.9)	17.0 (1.0)	17.1 (1.2)	17.8 (1.5)

Table 9 (cont.)

Group Number	Solar Elevation Angle (Degrees)								
	20	14	10	6	3	0	-2	-4	-6
21	12.1 (1.8)	13.5 (1.2)	14.8 (1.1)	15.7 (0.9)	16.4 (1.2)	17.4 (1.2)	17.3 (1.2)	17.4 (1.1)	17.4 (0.9)
22	11.7 (1.3)	12.7 (2.9)	14.1 (2.3)	15.8 (2.1)	16.5 (1.2)	17.0 (1.0)	17.2 (1.0)	17.1 (1.0)	17.3 (1.2)
23	12.0 (0.9)	13.3 (0.8)	13.6 (1.1)	14.5 (0.9)	15.5 (0.8)	16.4 (1.0)	15.9 (0.8)	15.3 (0.9)	14.9 (1.1)
24	12.0 (2.0)	13.4 (1.7)	14.4 (1.6)	15.5 (1.4)	16.3 (1.1)	17.0 (1.0)	17.3 (0.9)	17.0 (1.1)	17.2 (0.8)
25	12.0 (2.5)	14.9 (1.3)	15.4 (1.8)	16.6 (1.4)	17.4 (1.2)	18.4 (1.3)	18.2 (1.2)	18.2 (0.5)	19.1 (1.7)
26	11.6 (0.4)	13.6 (0.9)	14.2 (1.7)	16.2 (1.5)	17.4 (1.6)	18.1 (1.6)	18.2 (1.4)	17.7 (1.3)	17.5 (1.6)
27	15.6 (0.0)	16.6 (0.9)	15.4 (2.0)	16.7 (1.7)	17.6 (1.2)	18.4 (1.2)	17.8 (1.4)	17.3 (1.3)	17.3 (1.5)
28	12.0 (0.0)	13.7 (9.9)	14.5 (1.9)	16.9 (2.0)	17.8 (1.7)	18.6 (1.6)	18.8 (1.1)	19.9 (1.1)	18.9 (1.4)
29	11.5 (0.0)	13.8 (0.3)	13.5 (1.5)	14.9 (1.9)	17.0 (1.6)	17.6 (1.3)	17.4 (1.3)	17.6 (2.5)	16.5 (1.1)
30	9.6 (1.2)	12.3 (1.5)	14.0 (1.1)	15.4 (1.1)	16.3 (0.6)	17.6 (0.7)	17.6 (0.7)	17.4 (0.7)	17.0 (0.7)
31	12.5 (0.2)	13.6 (1.0)	14.1 (0.7)	15.1 (0.6)	15.8 (0.9)	16.6 (0.9)	15.0 (0.5)	14.4 (0.6)	16.2 (0.0)
32	11.2 (1.0)	13.0 (1.7)	14.4 (1.8)	15.8 (1.9)	16.3 (2.0)	17.1 (2.3)	17.4 (2.4)	17.9 (2.4)	18.4 (2.1)
33	18.8 (5.6)	19.5 (4.8)	20.2 (5.5)	23.2 (5.9)	27.1 (6.3)	29.9 (5.9)	23.4 (2.2)	22.5 (4.1)	24.4 (4.2)
34	25.2 (2.5)	28.4 (2.9)	32.1 (3.0)	36.9 (2.8)	41.1 (2.9)	34.7 (4.7)	23.4 (3.9)	20.6 (3.9)	21.7 (2.5)
35	19.2 (2.7)	22.6 (2.8)	25.0 (2.8)	29.1 (3.7)	33.0 (3.6)	32.7 (2.7)	24.2 (2.3)	23.2 (4.1)	21.3 (2.9)
36	16.8 (3.2)	20.4 (3.4)	23.5 (3.3)	26.5 (3.0)	29.3 (3.0)	29.6 (3.0)	25.3 (2.1)	22.7 (3.8)	21.1 (2.7)
37	18.4 (4.1)	19.2 (3.8)	21.5 (4.2)	24.2 (4.0)	27.5 (3.9)	28.3 (2.6)	24.2 (2.1)	19.7 (2.6)	19.9 (2.1)
38	14.7 (1.8)	16.3 (2.2)	17.6 (2.0)	20.2 (2.1)	22.7 (1.9)	24.7 (2.4)	24.8 (2.1)	22.2 (2.3)	21.7 (1.7)
39	14.4 (2.3)	15.6 (2.6)	17.1 (2.5)	18.4 (2.2)	20.0 (2.6)	21.8 (2.4)	22.1 (1.4)	20.2 (1.6)	19.7 (1.1)
40	13.4 (1.5)	14.5 (1.8)	15.5 (1.4)	17.4 (1.8)	18.7 (1.5)	19.6 (1.5)	19.7 (1.4)	19.1 (1.6)	19.3 (2.3)

Table 10. Averaged Values of DBA for the Groups in Table 7. The Brackets Indicate Those Values That Have Been Estimated. Note That the Standard Deviations Have Not Been Calculated for DBA

Group Number	Solar Elevation Angle (Degrees)								
	20	14	10	6	3	0	-2	-4	-6
1	[-5.2]	-5.1	-5.3	-0.4	0.9	3.5	3.6	3.2	2.0
2	[-7.5]	-7.3	-5.7	-5.1	-2.0	-0.6	0.9	0.7	0.2
3	-8.5	-10.2	-8.1	-5.4	-3.4	-0.6	-0.9	-1.9	-3.7
4	-11.1	-9.2	-7.6	-4.9	-2.8	-0.5	-1.2	-2.2	-6.3
5	-9.6	-7.1	-6.5	-5.0	-3.1	-1.0	-1.0	-0.9	-4.3
6	-8.5	-7.6	-6.5	-4.2	-2.0	0.1	1.0	-0.6	-1.7
7	-8.3	-7.6	-6.1	-5.1	-3.3	-1.0	-0.4	-1.5	-3.8
8	-8.0	-8.7	-7.5	-5.9	-4.3	-1.5	-1.2	-2.0	-4.0
9	-10.3	-9.1	-7.5	-6.1	-3.6	-1.3	-0.5	-2.5	-4.0
10	-8.9	-8.9	-7.9	-5.8	-3.7	-1.4	-0.7	-1.1	-4.8
11	-8.5	-8.0	-6.5	-5.2	-3.1	-1.1	-0.2	1.9	-4.3
12	-9.7	-8.6	-7.0	-5.3	-3.7	-1.6	-0.9	-2.2	4.0
13	-6.0	-7.8	-6.3	-5.8	-4.0	-2.2	-1.4	-2.9	-4.0
14	-9.3	-8.3	-6.6	-4.4	-3.9	-1.8	-1.9	-3.4	-6.6
15	-10.2	-6.8	-6.0	-5.8	-4.2	-2.7	-2.4	-2.5	-6.1
16	[-10.0]	-9.4	-8.3	-6.1	-4.0	-1.7	-1.0	-2.0	-6.7
17	-12.5	-9.1	-7.5	-5.0	-4.1	-2.6	-1.9	-4.4	-4.4
18	[-9.0]	-9.0	-8.3	-6.0	-4.5	-3.0	-2.3	-4.7	-7.3
19	[-8.0]	-7.6	-7.5	-6.8	-6.0	-2.0	-2.4	-3.7	[-6.5]
20	-11.4	-9.2	-7.2	-5.6	-3.8	-2.0	-1.8	-3.8	-6.2
21	-10.1	-8.1	-6.5	-5.4	-4.0	-1.4	-1.3	-3.0	-7.0
22	-10.1	-8.8	-7.3	-3.6	-1.9	-1.5	-1.5	-3.2	-8.2
23	[-10.0]	-7.8	-7.1	-5.9	-4.2	-2.1	-1.4	-4.9	-9.1
24	-12.2	-7.0	-6.8	-5.2	-3.9	-2.0	-1.4	-4.2	-10.3
25	[-9.0]	-7.0	-6.9	-6.1	-4.5	-2.3	-2.4	-3.2	-7.3
26	-8.8	-8.8	-7.6	-6.1	-4.9	-3.4	-2.3	-3.2	-7.8
27	[-6.0]	-4.0	-7.0	-5.9	-4.6	-2.6	-2.2	-3.4	-4.0
28	[-7.0]	-9.7	-7.6	-4.7	-3.0	-1.5	-0.5	-1.6	-5.7
29	[-10.0]	-6.6	-6.9	-6.2	-3.5	-1.9	-1.9	-2.7	[-8.0]
30	-12.6	-10.0	-7.4	-5.8	-4.6	-2.0	-2.1	-4.1	-10.2
31	-9.4	-9.4	-8.0	-6.6	-4.5	-2.5	-2.8	-6.2	-2.8
32	-10.7	-9.0	-7.4	-6.0	-5.4	-3.7	-2.3	-4.0	-7.4
33	-6.4	-6.3	-5.3	-2.7	1.0	5.6	1.7	-0.2	-0.8
34	-5.8	-3.5	0.4	5.1	9.7	9.6	2.5	-1.5	-4.3
35	-7.8	-1.8	-0.6	2.3	5.6	8.2	2.5	1.7	-4.0
36	-7.1	-3.7	-1.6	0.6	3.2	5.3	3.0	0.6	-3.0
37	3.9	-3.9	-2.3	-0.7	2.1	4.4	3.0	-2.0	-6.1
38	-9.4	-7.7	-6.2	-3.4	-1.0	-1.6	2.4	-1.0	-4.1
39	-7.4	-6.6	-5.1	-3.8	-2.3	-0.6	0.9	-1.3	-5.6
40	-10.0	-8.7	-7.3	-5.6	-3.9	-2.3	-1.6	-3.5	8.4

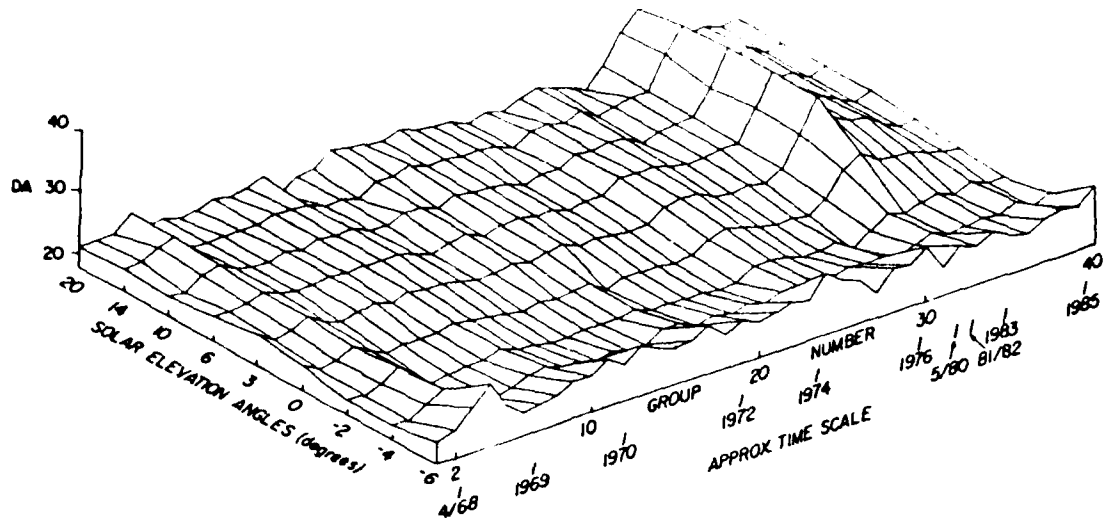

Figure 10. 3-D Plot of DA for the Groups Given in Table 7. For Reference, the Approximate Time Scale Is Given Along the Group Number Axis

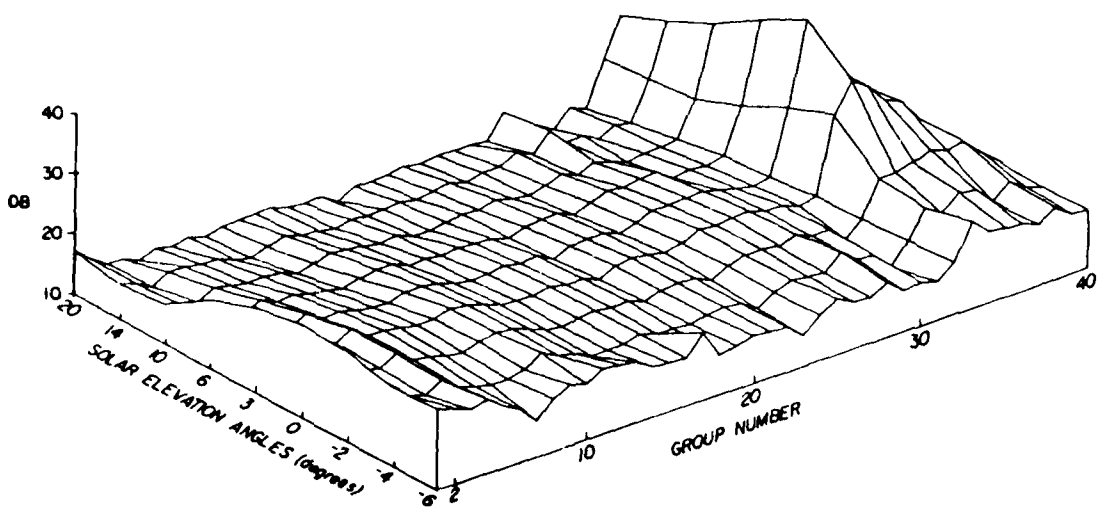

Figure 11. 3-D Plot of DB for the Groups Given in Table 7

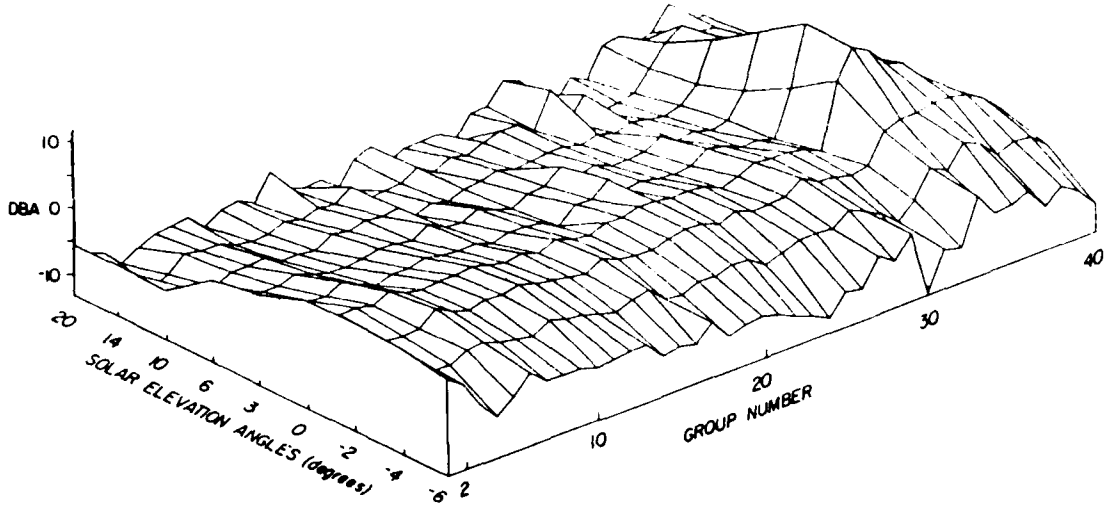

Figure 12. 3-D Plot of DBA for the Groups Given in Table 7

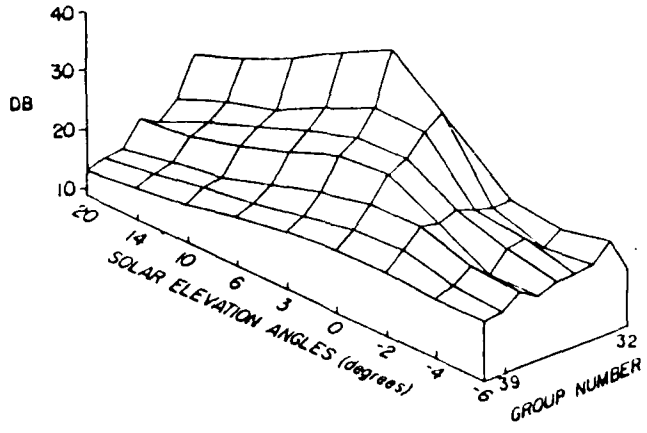

Figure 13. 3-D Plot Showing the Decline of DB During the El Chichon Period

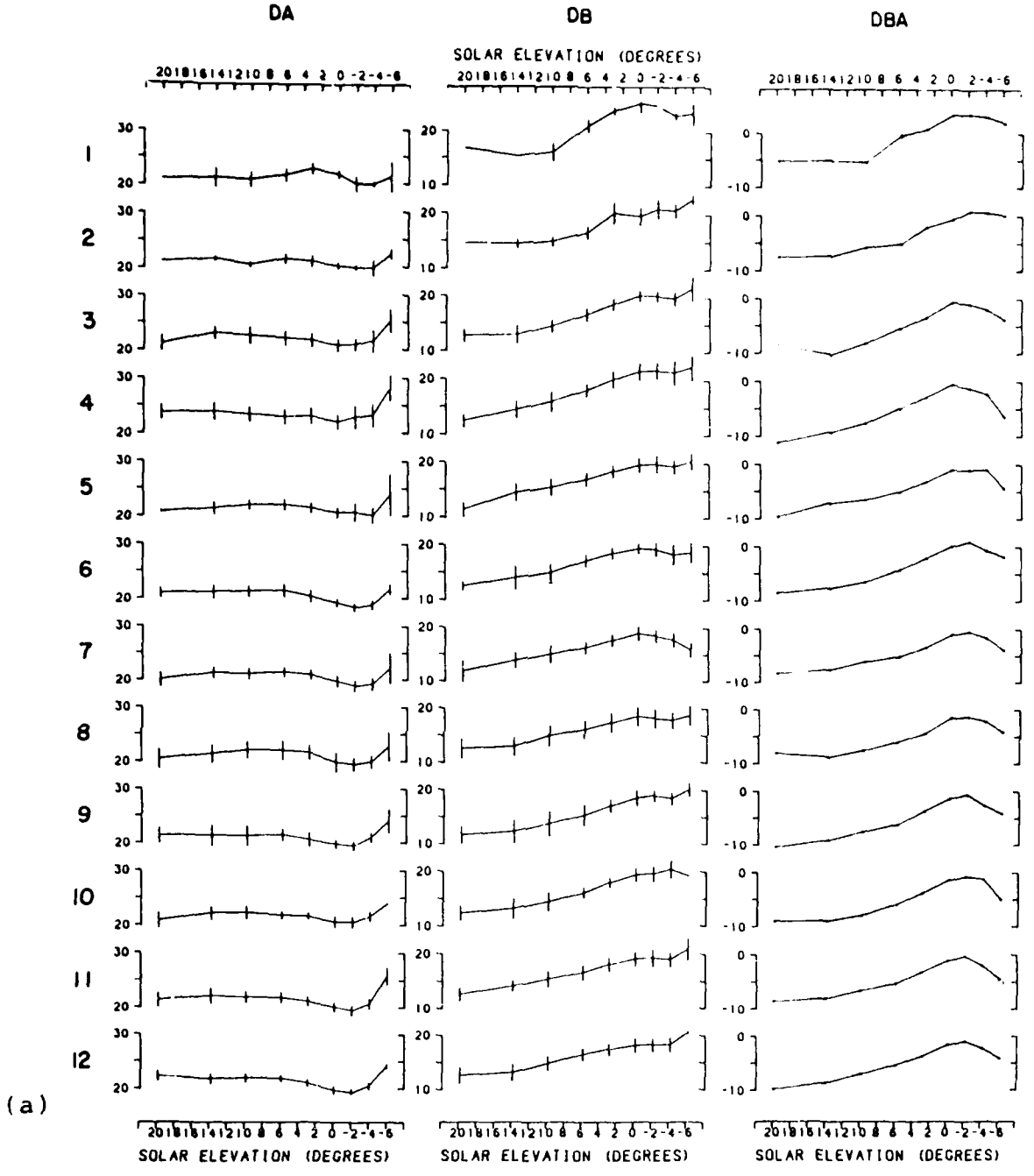

Figure 14. Staggered Plots of DA, DB, and DBA, in Degrees, as a Function of Solar Elevation Angle for the Group Numbers (a) 1 to 12, (b) 13 to 26, and (c) 27 to 40 in Table 7. The Standard Deviations Have Been Indicated on the DA and DB Plots

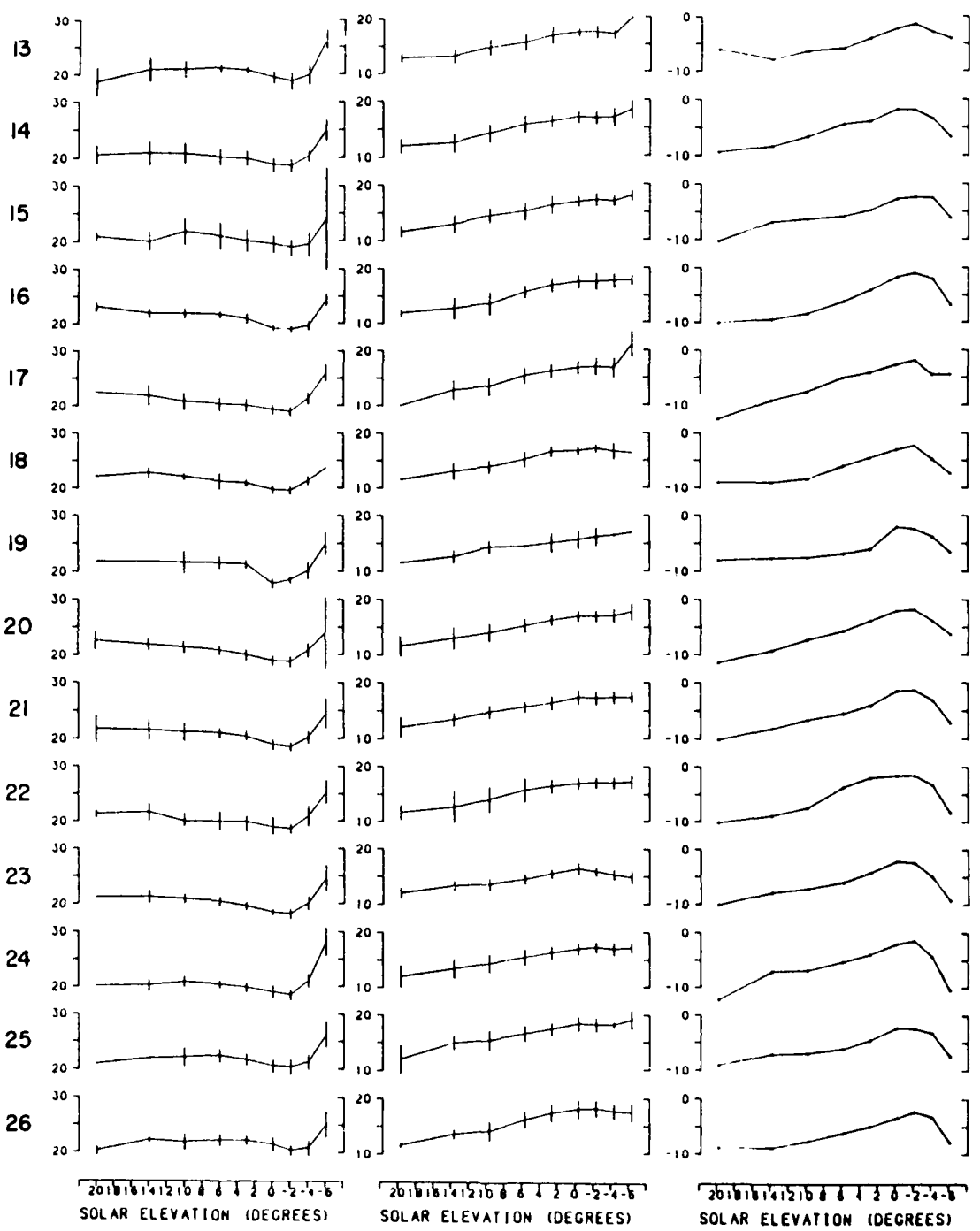

(b)

Figure 14. (cont.)

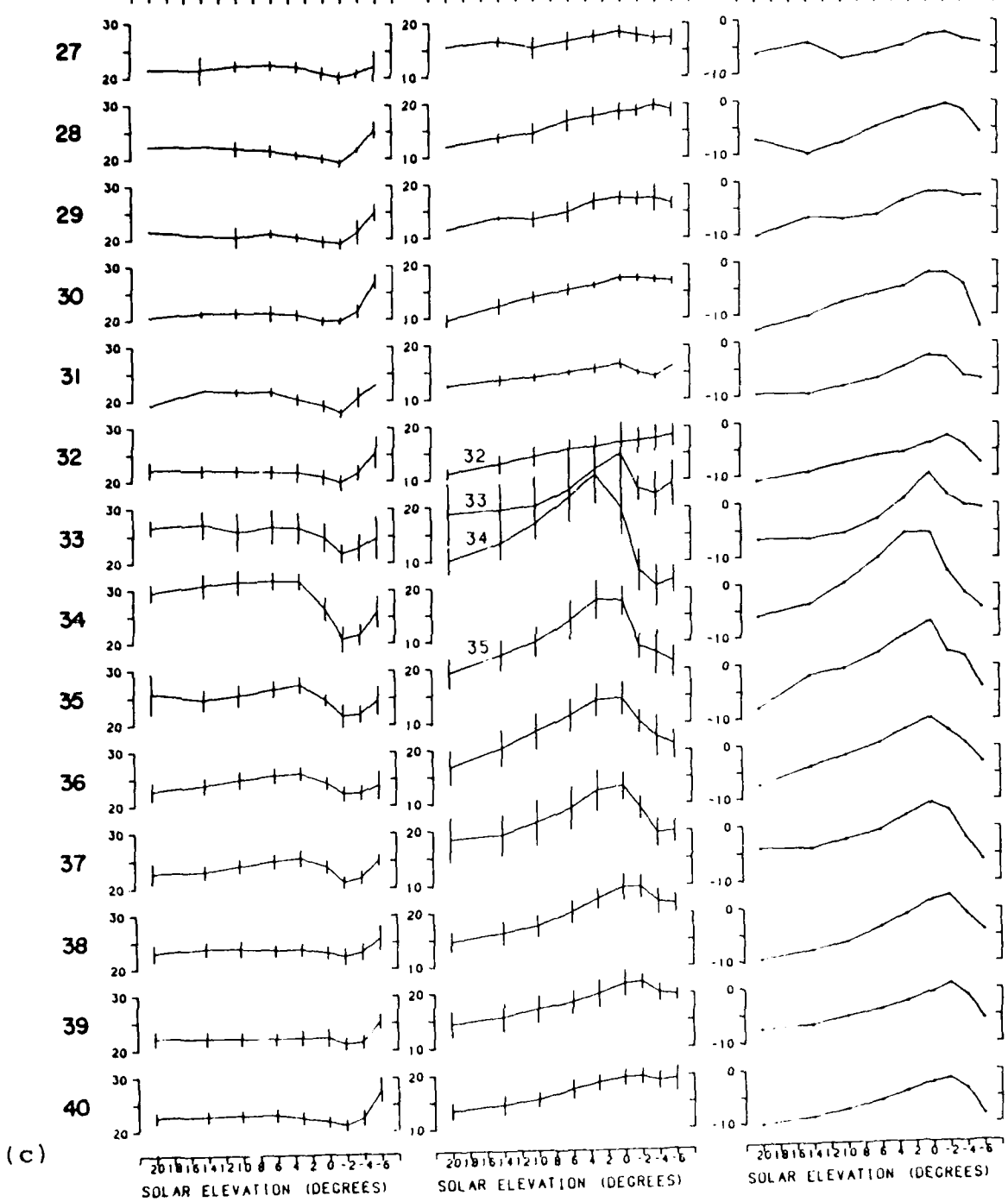

Figure 14. (cont.)

6.3 Discussion of the Plots

The 3-D plots are more instructive than the staggered plots because they bring out general trends in the data very well. The flat valley in DA shortly after sunset and before sunrise (i.e. H between 0 and -4 degrees) is a pronounced feature throughout all of the data. Prior to the El Chichon period, the surfaces of DA and DB have about the same smoothness, despite the higher accuracy of the DA measurements. Only the values of DB in the first group (if the omitted observations 1 to 12 in Table 7 are included) seem to have a significant deviation. This is probably due to the remnants of earlier volcanic eruptions.

In the El Chichon period, DB rises about twice as much as DA. The high values of DB extend not only to a solar elevation angle of 3 degrees, but sometimes to 0 or -1 degrees. Figure 13 indicates that the values of DB were near normal by 1986, just like the stratospheric aerosol counts and CR data (Figure 9).

The surface of DBA is generally a flat ridge that reaches a maximum at a solar elevation angle of 0 degrees. During the El Chichon period however, a peak protrudes over the ridge. Also the surface is slightly rougher than those of DA and DB. The edges are especially rough because fewer observations were taken at -6 and 20 degrees. Incidentally, the expression

$$DA + DB - 40$$

produces, even for the El Chichon condition, a very similar course as DBA.

One observation can be made from the staggered plots (see Figure 14): the standard deviations of DA and DB in the El Chichon period are larger than those in nonvolcanic periods. This suggests that the day-to-day movement of neutral points is greater during highly volcanic conditions. No explanation for this behavior is offered at the current time.

In an attempt to find a relationship between the details provided by the CR and the behavior of the neutral points, a number of pre-El Chichon groups in Table 7 have been separated according to high and low conditions of CR (see Table 11). Group a is a comparison between neutral point data taken after the arrival of the Fuego dust clouds of 1971 and 1974 (high CR conditions), and background values (low CR conditions). In groups b through f, fall/winter measurements (high CR conditions), of the neutral points are compared with those for the spring/summer (low CR conditions). Here it should be noted that group numbers 32 through 40 in Table 7 were not included in the analysis because these data were dominated by presence of the El Chichon dust cloud.

For group a, no significant differences were found between the values of DA, DB and DBA in high CR conditions and those in low CR conditions. In light of this, we feel that the Fuego dust clouds of 1971 and 1974 were probably too diffuse to effect the position of the neutral points.

Table 11. "Supergroups" for High and Low CR Conditions

Supergroup	High CR			Low CR			Behavior of Neutral Points in High vs Low CR Conditions
	Reason for High CR	Groups Averaged	Number of Sets	Reason for Low CR	Groups Averaged	Number of Sets	
a	Presence of Dust Clouds from the 1971 and 1974 Eruptions of Fuego	17, 26	44	Background Stratospheric Aerosol during the Fall/Winter of 1972-1974	18, 20, 22	141	Small Differences DA, DB, and DBA
b	1968 Fall/Winter	1, 3	39	Weak Spring/Summer Effect of 1968	2	20	Similar Seasonal Movements of DA, DB, and DBA: See Figure 15 for the Average Seasonal Change in DBA
c	1975-1977 Fall/Winter	28, 30	28	Strong Spring/Summer Effect of 1976 (Post Fuego)	29	10	
d	1972-1974 Fall/Winter Background Stratospheric Aerosol	18, 20, 22	141	Spring/Summer Effect of 1972-1974	19, 21, 23	64	
e	1968-1969 Fall/Winter	3, 5, 9, 10	129	Strong Spring/Summer Effect of 1969	6, 7, 8	88	Seasonal Movements of DA, DB, and DBA But Only Partial Agreement with b-d (See Figure 15)
f	1969-1971 Fall/Winter	9, 14	97	Weak Spring/Summer Effect of 1970	12, 13	60	

In contrast, groups b through f indicate that there is a seasonal movement of DA and DB. In particular, groups b, c and d yield essentially the same differences between fall/winter values of DA, DB and DBA and spring/summer measurements (illustrated for DBA in Figure 15). Groups e and f, on the other hand, differ from groups b through d in various aspects. Unfortunately, we have no explanation for the behavior of groups e and f and consequently, feel it would be premature to draw conclusions from the results in Figure 15.

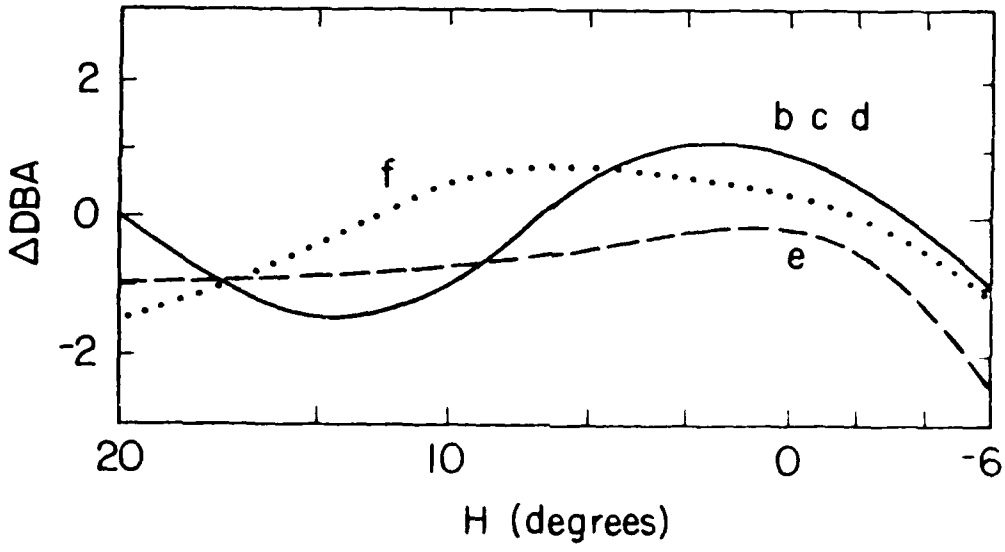

Figure 15. ΔDBA as a Function of Solar Elevation Angle for Supergroups b through f

6.4 Comparison with Other Measurements

6.4.1 Data from Mauna Loa, Hawaii during the El Chichon Period

The El Chichon dust cloud reached an unusually great altitude over the tropics shortly after the eruption. Lidar returns peaked at 25 to 27 km, compared with 17 to 22 km on most days in the northern midlatitudes, and the optical thicknesses were up to twice as large also. From his photopolarmetric measurements during July and August of 1982 at Mauna Loa, Hawaii, Coulson[11] has derived neutral point data. His data exhibit much more pronounced features (see Figure 16) when compared with the values in Figure 3. In particular, DB rose to 60 degrees at a solar elevation of 4 degrees, descended momentarily to about 0 degrees at the time when the solar rays passed through the aerosol layer tangentially (i.e. at a refracted solar elevation angle of 0 degrees), and ascended again. To honor the late Kinsell L. Coulson, who first measured these sunset features, we propose to name them Coulson features. In short, Coulson features are characterized by a minimum value of DB near sunset (or sunrise) and an increase at negative solar elevation angles.

In our observations, good examples of the Coulson features seem to have occurred only on a few evenings between October 1982 and January 1983. Four of the best cases are shown in Figure 17; their similarity to the Hawaii results

[11] Coulson, K.L. (1983) Effects of the El Chichon volcanic cloud in the stratosphere on the polarization of light from the sky, Appl. Opt. 22: 1036-1050.

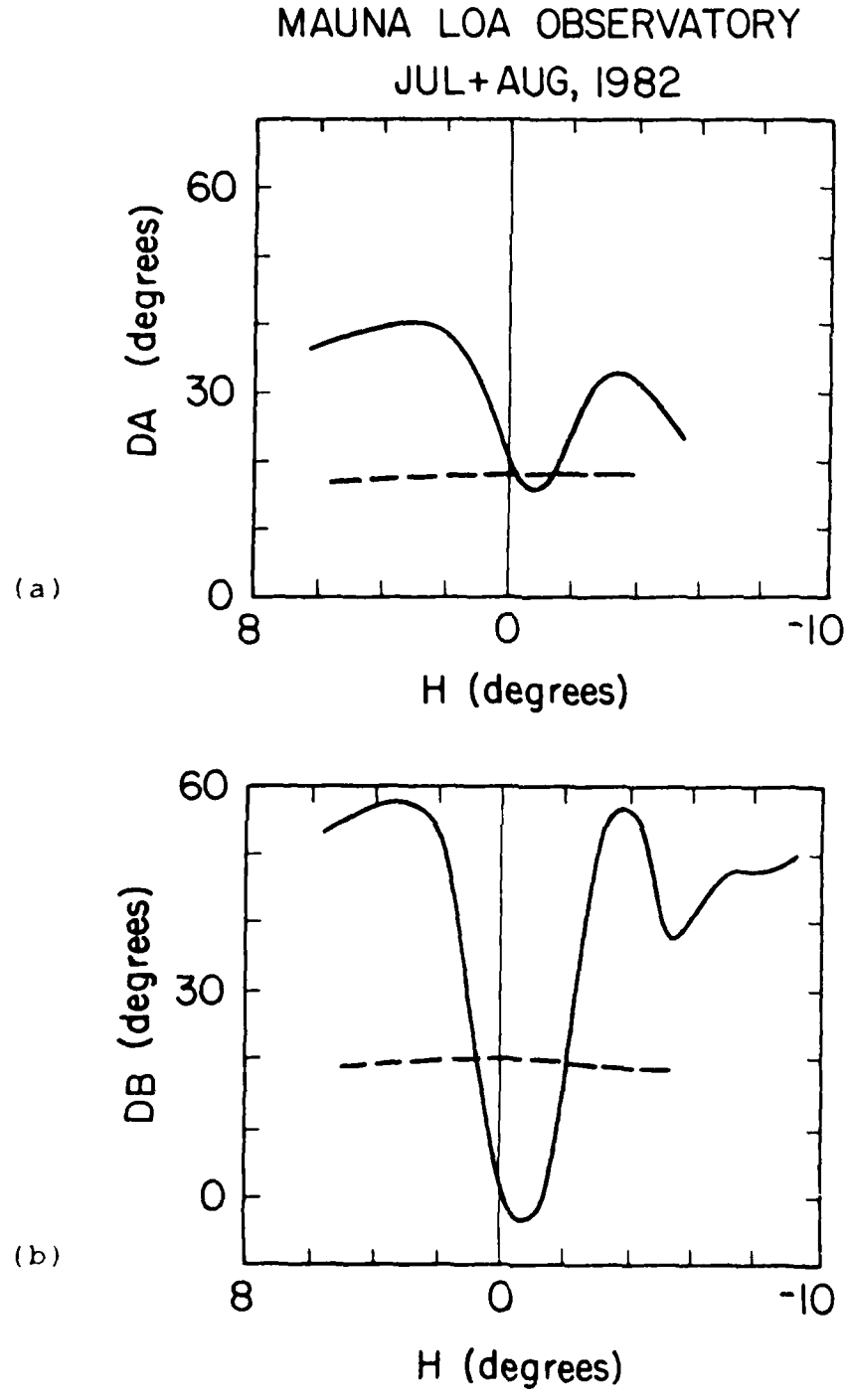

Figure 16. Values for (a) DA and (b) DB During the Very High Volcanic Turbidity Conditions at Mauna Loa, Hawaii (Adapted from Figures 14 and 15 of Coulson[11]). The Dashed Lines are Background Values

COULSON FEATURES

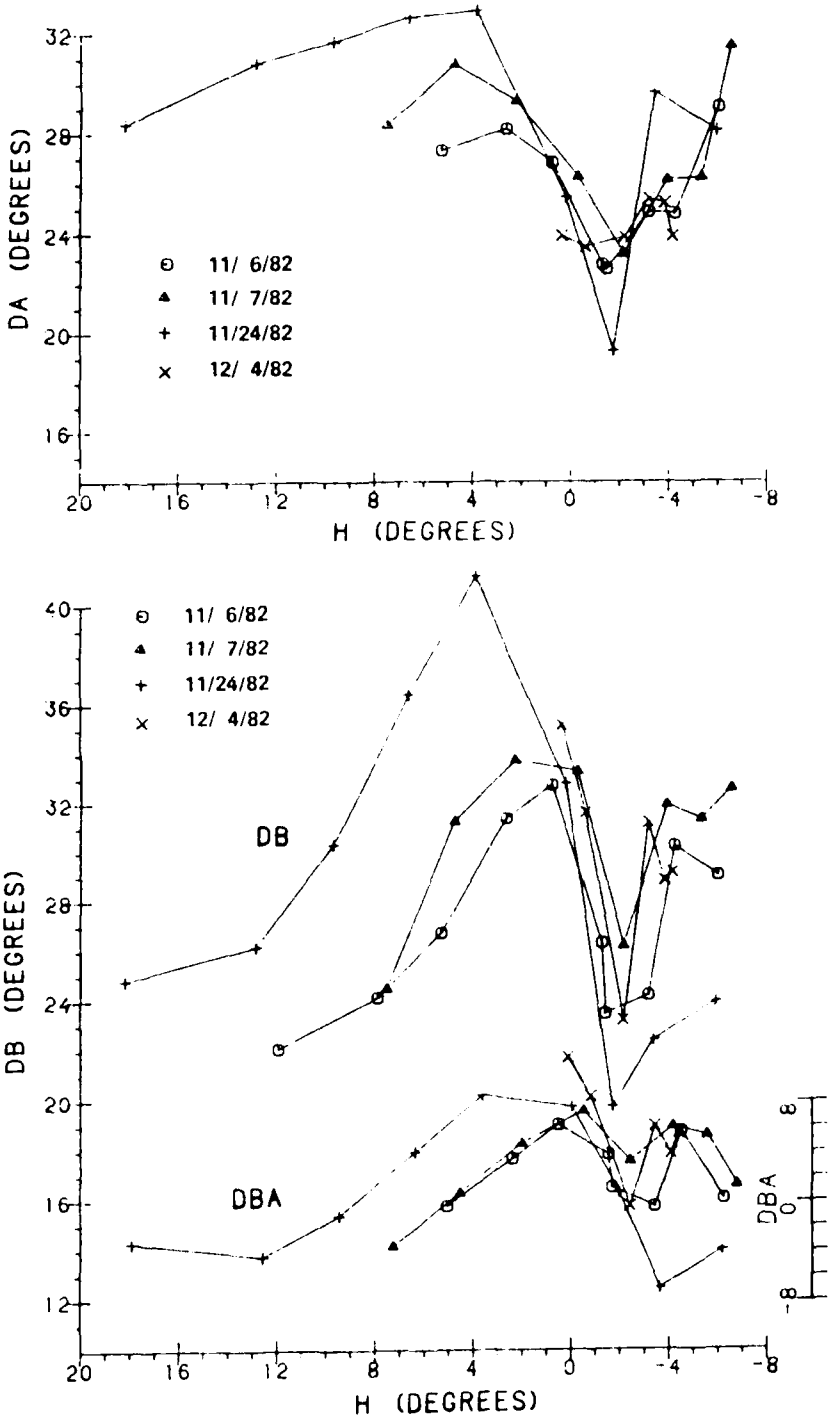

Figure 17. Examples of the Coulson Features in Our Data for Selected Days Between November 6, 1982 and December 4, 1982

is evident. Weaker Coulson features were also observed between July and September of 1983, but under less favorable observation conditions. Interestingly, our Coulson features seem to coincide with the time periods when an aerosol layer was observed above the normal El Chichon dust cloud. The aerosol layer, which may be the formation of sulfuric acid droplets from sulfur dioxide gas of the El Chichon eruption, has been seen at altitudes of up to 40 km (at northern mid-latitudes) in the European lidar measurements of Adriani et al.[12] and the satellite data from Clancy[13]. Unfortunately, it is too difficult to confirm a direct relationship between the Coulson features and the high aerosol layer. That is, the lidar and the satellite data are for different longitudes and therefore, the west-to-east movement of the dust cloud must be accounted for when comparing the times of observed Coulson features and the high aerosol layer.

6.4.2 Historical Data

There are many series of neutral point observations, the first dating back to 1854. Most, however, were of short duration and nearly all cover only the solar elevation range from 8 degrees to -5 degrees. Furthermore, it is difficult

12. Adriani, A., Condeduti, F., Gobbi, G.P., Irgi, R., and Fiocco, G. (1984) The El Chichon Aerosol cloud observed by lidar in Frasacati, March 1982 April 1984: backscattering and extinction, Proceedings of the International Radiation Symposium Perugia, Italy 21 28 August 1984, A. Deepak Publishing, Hampton, Va.
13. Clancy, R. (1986) El Chichon and "mystery cloud" aerosols between 30 and 50 km: global observations from the SME visible spectrometer, Geophys. Res. Lett. 13:937-940.

to compare series of observations because few are averaged or are on conforming plots. Therefore, it was desirable to assemble the historic data into a unified format.

In the course of the present work, plots in the form of Figures 2 and 3 were produced for most of the historical data. Depicted in the left part of Figure 18 are the results from Germany (Jensen[14]) for the years that followed the eruptions of Mt. Soufriere and Mt. Pelee in the spring of 1902. The peaks of DA and DB are the same as in our El Chichon data, but there is no indication of a Coulson type increase in the value of DB after sunset. Although not shown in this report, Coulson features also were not observed after the Katmai eruption of 1912 in Alaska. The absence of the Coulson features in these historical data was probably because the high layers of volcanic dust did not exist. The right part of Figure 18 gives Jensen's values of DA and DB for non-volcanic periods. These values indicate that in 1907, when the optical thickness of the Soufriere and Pelee dust clouds had decreased to about 0.01, DA was nearly normal but DB was still six degrees higher than values in non-volcanic periods.

14. Jensen, C. (1937) Die Verfolgung der neutralen Punkte der atmospharischen Polarisation in Arnsberg i.w. wahrend eines Zeitraums von 19 Jahren, Meteor. Z. 54: 90-97.

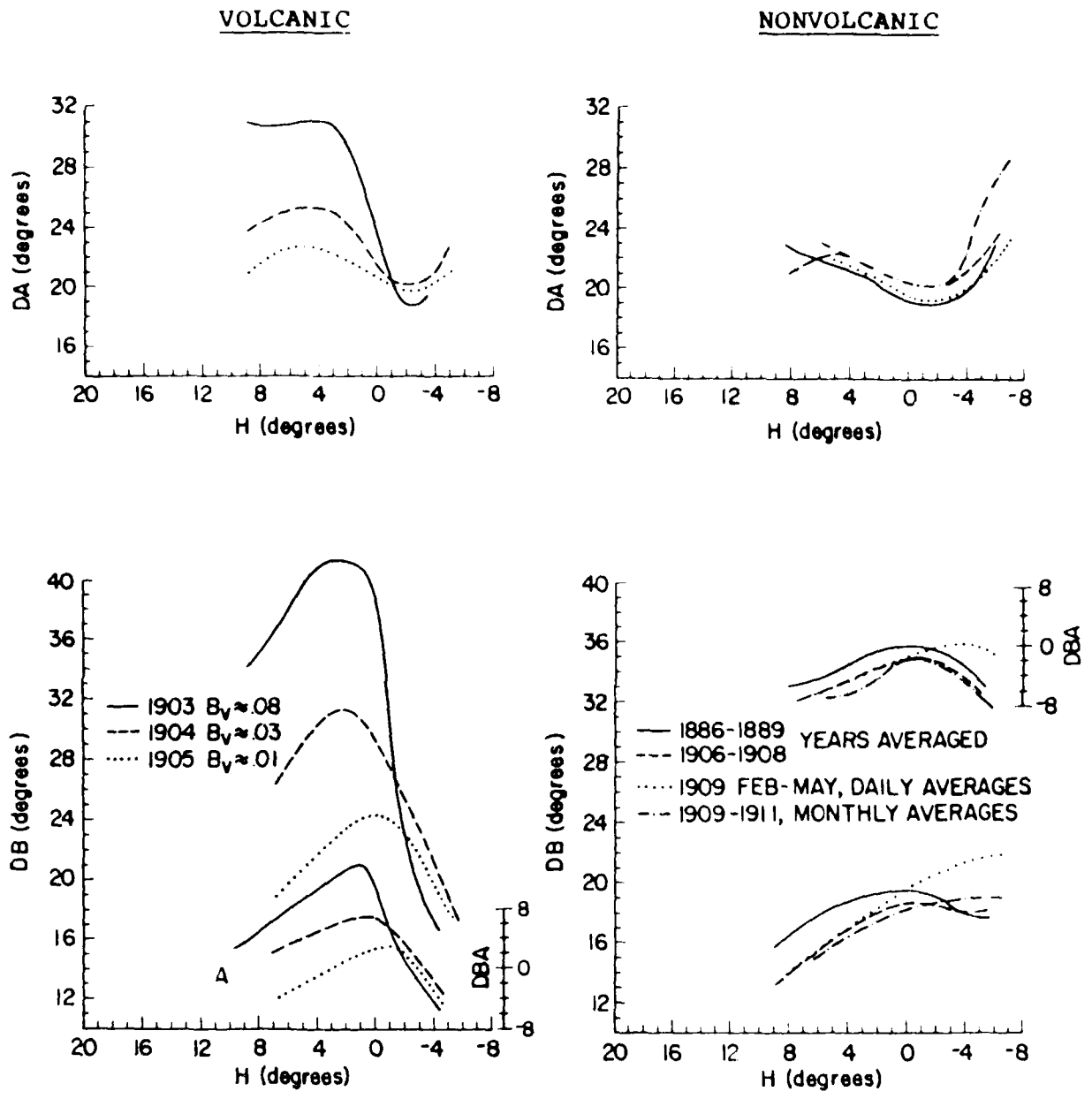

Figure 18. Neutral Point Data (left) After the Eruptions of 1902 and (right) During Nonvolcanic Periods. After Jensen[14]

7. Summary

The Arago and Babinet neutral points, defined as the distances *DA* and *DB* from the antisolar and solar angle respectively, were obtained at Bedford and Lexington, Massachusetts, for most of the years between 1968 and 1986. Neutral point data at nine fixed solar elevations formed the basis for the present effort. Many observations extend to solar elevations of 20 degrees and -6 degrees. The data have been checked carefully for errors and combined with additional measurements of atmospheric turbidity, turbidity type, cloud cover, solar aureole and twilight color ratio. The resulting database consists of a total of about 1300 morning and evening observation sets.

The main purpose of the present effort was to assess the seemingly undetectable effects of the two moderate volcanic dust veils of Fuego in 1971 and 1974, and the large effect after the El Chichon eruption of 1982. Prior to this, the effect of tropospheric turbidity on the neutral points was determined using the data preceeding 1980. The neutral points were then corrected accordingly. In addition, the effects of snow covered ground and sea surface reflection of sunlight on the neutral points were found to be negligible.

The data set was subdivided into 40 groups for plotting purposes. The grouping was based primarily on stratospheric aerosol data, but the details of the twilight color ratio measurements were also considered. A number of observations were made from the the plots:

1) the surface of DA contains a pronounced flat valley near a solar elevation angle of -2 degrees

2) for the pre-El Chichon period, the 3-D plot of DBA has a much rougher surface than that of DA and DB

3) the El Chichon effect on the data took at least three years to subside

4) the grouping of the data according to high and low values of CR seems to have yielded signatures for the spring to fall effect

5) the weak eruptions of Fuego were not detectable

6) the standard deviations of the neutral point data in the El Chichon period were larger than those in non-volcanic periods

Our data were then compared with measurements made by other researchers. In general, the increase of DB and DA during the El Chichon episode was smaller than it was initially in the tropics. During the Fall of 1982 and early Winter of 1983 however, the high values sometimes continued at negative solar elevation angles, with a sharp minimum intervening at actual sunset or sunrise (that is, at 0 degrees refracted solar elevation angle). These "Coulson features," which seem to have been caused by the especially great height of the El Chichon dust cloud and the reduced volcanic turbidity at lower altitudes, were not observed after the eruptions of 1902 and 1911, probably because the high layers of volcanic dust did not exist.

References

1. Sekera, Z. (1956) Recent developments in the study of the polarization of skylight, in Advances in Geophysics, Academic Press, Inc., New York, 3:43-104.

2. Jensen, C. (1957) Die Polarisation des Himmelslichtes, in Handbuch der Geophysik, Borntraeger, Berlin, 8:527-620.

3. Chandrasekhar, S. (1950) Radiative Transfer, Oxford University Press.

4. Coulson, K.L., Dave J.V., and Sekera Z. (1960) Tables Related to Radiation Emerging from a Planetary Atmosphere with Rayleigh Scattering, University of California Press, Berkley and Los Angeles.

5. Holzworth, G., and Rao C.R.N. (1965) Studies of skylight polarization, J. Opt. Soc. Am. 55:403-408.

6. Fraser, R.S. (1968) Atmospheric neutral points over water, J. Opt. Soc. Am. 58:1029-1031.

7. Neuberger, H. (1941) The influence of the snow cover on the position of Arago's neutral point, Bull. Am. Meteorol. Soc. 22:348-351.

8. Volz, F.E. (1984) Volcanic turbidity, skylight scattering functions, and sky polarization and twilight in New England during 1983, Appl. Opt. 23: 2589-2593.

9. McCormick, M.P., Swissler, T.J., Fuller, W., Hunt H., and Osborn, M.T. (1984) Airborne and ground-based lidar measurements of the El Chichon stratospheric aerosol from 90 degrees N to 56 degrees S, Geof. Int. 23:187-221.

10. Hoffman, D., and Rosen, J. (1986) Atmospheric effects, SEAN Bull. 11:No.5, 20.

11. Coulson, K.L. (1983) Effects of the El Chichon volcanic cloud in the stratosphere on the polarization of light from the sky, Appl. Opt. 22: 1036-1050.

12. Adriani, A., Condeduti, F., Gobbi, G.P., Ligi, R., and Fiocco, G. (1984) The El Chichon Aerosol cloud observed by lidar in Frasacati, March 1982-April 1984: backscattering and extinction, Proceedings of the International Radiation Symposium Perugia, Italy 21-28 August 1984, A. Deepak Publishing, Hampton, Va.

13. Clancy, R. [illegible] 1986: El Chichon and "mystery cloud" aerosol between 40 and 50 km: global observations from the SME visible spectrometer, Geophys. Res. Lett. [illegible].

14. [illegible] der neutralen Punkte [illegible] Arnsberg i.w. [illegible] Jahren, Meteor. Z. 54: [illegible].

Appendix

Additional Parameters in the Database

A.1 Turbidity Type

The Turbidity Type (TT) is a qualitative observation that gives a sensitive indication of the size distribution in the radius range from about 0.2 to 2 microns. The observations were made at a solar elevation angle of about 25 degrees and require the use of brown sunglasses, both for reduction of glare and for the supression of molecular scattering. Cold air inflow is often characterized by strong forward scattering and by blue sky farther than three degrees from the sun (TT=1.3). By contrast, hazier skies may exhibit a nearly constant brightness (and color) up to 20 degrees away from the sun (TT=2.0). The turbidity type is stored in the database as TT x 10.

A.2 Solar Aureole

Normally, the sky around the sun is very bright due to the forward scattering by dust particles and pollen. These particles typically have diameters between about 2 and 30 microns, comparable in size to fog and cloud droplets. As shown by observations in the course of a clear day, the dust and pollen are lifted by wind and turbulence from the surface industry and road traffic. They are kept afloat by convection.

Rather crude estimates of aureole brightness (A) were obtained until 1974 by looking at the sky about 0.5 degrees from the sun, from the shadow of a distant roof. If with the unaided eye, the aureole was not glaring or was barely glaring, the designation was A=0. If one sunglass was needed to reduce glare sufficiently, then A=1, etc. Sky conditions with cirrus veils can easily be recognized by this method because these ice crystals have very strong forward scattering up to 0.2 degrees from the sun. The brownish sunglasses used to make the measurements had an optical density between 1.0 and 1.3 for wavelengths between 0.45 and 0.55 microns, and 0.5 at wavelengths of 0.64 and 0.35 microns.

A.3 Color Ratio

The logarithm of the color ratio (LCR) is derived from continuous recordings during twilight of the sky's intensity at wavelengths of 0.50 microns (G) and 0.85 microns (U) at 20 degrees elevation in the solar azimuth. At four to five degrees solar depression angle, the intensity at U responds most strongly to the amount of volcanic aerosol. The U intensity will be lower however, if clouds at, or beyond the sunset horizon hide the earth shadow so as to reduce the illumination of the stratospheric aerosol (as often evidenced by crepuscular rays). At 0.50 microns, the solar illumination of the stratosphere is much weaker during the twilight and effects by the volcanic aerosol and cloud shadows are

barely recognizable. Therefore, the intensity decrease at G serves as stable reference for that at U:

$$LCR=\log_{10}\left[(U/G)_{4\ \text{degrees}}/(U/G)_{0\ \text{degrees}}\right].$$

It follows that for periods of a few months duration, the upper level of LCR corresponds to twilights undisturbed by distant clouds (whether volcanic or not), while reduced LCR could indicate such cloud disturbances. Because the neutral point observations were made in white light ($\lambda_{\text{eff}} = 0.55$ microns), it is unlikely that they will respond to the cloud disturbance indicated by the LCR values.

END

FILMED

MARCH, 1988

DTIC